



LTE-based passive radars and applications: a review

Prabhat Kumar Rai, Abhinav Kumar, Mohammed Zafar Ali Khan & Linga Reddy Cenkeramaddi

To cite this article: Prabhat Kumar Rai, Abhinav Kumar, Mohammed Zafar Ali Khan & Linga Reddy Cenkeramaddi (2021) LTE-based passive radars and applications: a review, International Journal of Remote Sensing, 42:19, 7489-7518, DOI: [10.1080/01431161.2021.1959669](https://doi.org/10.1080/01431161.2021.1959669)

To link to this article: <https://doi.org/10.1080/01431161.2021.1959669>



© 2021 The Author(s). Published by Informa UK Limited, trading as Taylor & Francis Group.



Published online: 26 Aug 2021.



Submit your article to this journal [↗](#)



Article views: 278



View related articles [↗](#)



View Crossmark data [↗](#)

LTE-based passive radars and applications: a review

Prabhat Kumar Rai^a, Abhinav Kumar^a, Mohammed Zafar Ali Khan^a
and Linga Reddy Cenkeramaddi ^b

^aDepartment of Electrical Engineering, IIT, Hyderabad, India; ^bThe ACPS Research Group, Department of Information and Communication Technology, University of Agder, Grimstad, Norway

ABSTRACT

This paper provides an overview of the most recent passive radars based on long-term evolution (LTE). To begin, this paper investigates the various characteristics and requirements of 4 G LTE signals for radar, taking performance aspects such as range, velocity, range resolution, and velocity resolution into account. An ambiguity function analysis is performed on a measured LTE signal using the synchronization and reference signal components to evaluate key performance parameters such as Doppler and range characteristics. We also discuss how LTE passive radar can be used in a variety of applications. The detailed analysis of the LTE downlink signal, its structural overview, and the effect on cross- and self-ambiguity functions are all discussed. The paper investigates related standard development proposals, with a focus on performance evaluation criteria for existing passive radar technologies. As a result, this survey paper serves as a starting point for evaluating the performance of current and future passive radar innovations, including an emerging 5 G radar.



ARTICLE HISTORY

Received 15 May 2021

Accepted 18 July 2021

1. Introduction & motivation

Passive radar systems are a type of radar system that detects and tracks targets in the environment by processing reflections from non-cooperative sources of illumination, such as commercial broadcast and communications signals. The use of passive radar to detect aircraft targets dates back to 1935, when Sir Robert Watson-Watt conducted a bi-static experiment at Daventry using the illumination from the shortwave of 49 m wavelength BBC Empire transmitter to detect a Heyford bomber aircraft at a short distance of 8 km Swords (1986), Jack. Gough and Great Britain (1993). Long-term evolution (LTE) is the state-of-the-art wireless communication technology that delivers last-mile broadband cellular connectivity. Bandwidth range of LTE signals varies from 1.4 to 20 MHz with high range resolution and velocity resolution as compared to global system for mobile communications (GSM) and other existing cellular network signals. The wider frequency band of 800–3500 MHz, which supports both frequency division duplex (FDD) and time division duplex (TDD), and global coverage of LTE signals make passive radar configuration both feasible and accessible. Further, LTE utilizes orthogonal frequency division

CONTACT Linga Reddy Cenkeramaddi  linga.cenkeramaddi@uia.no  The ACPS Research Group, Department of Information and Communication Technology, University of Agder, Grimstad, 4879, Norway

© 2021 The Author(s). Published by Informa UK Limited, trading as Taylor & Francis Group.

This is an Open Access article distributed under the terms of the Creative Commons Attribution-NonCommercial-NoDerivatives License (<http://creativecommons.org/licenses/by-nc-nd/4.0/>), which permits non-commercial re-use, distribution, and reproduction in any medium, provided the original work is properly cited, and is not altered, transformed, or built upon in any way.

multiple access (OFDMA) and its ambiguity function produces lower side-lobes. Hence, all these mentioned properties make the LTE signals a strong candidate for the passive radar systems (Raja Abdullah et al. 2015; Salah et al. 2013).

The utilization of LTE signals for applications in radar systems has been explored in Salah et al. (2013). Further, in Evers and Jackson (2014a), LTE signal-based radar exploiting the properties of OFDM has been considered. The digital signalling in LTE with low error-rate decoding makes it a good contender for passive radars. Further, the OFDM in LTE signal has demonstrated efficacy in target identification based on Fourier analysis/Frequency analysis. Previous works on FM radio, WiFi, television station (DVB-T) broadcasting in UHF/VHF frequency bands for passive radar purpose have been presented in Coleman, Watson, and Yardley (2008), Kuschel et al. (2008), and Mueller et al. (2007).

There is a growing demand for Unmanned Aerial Vehicles (UAVs), Unmanned Ground Vehicle (UGVs), and autonomous robots in recent years. LTE passive radars have shown to be highly useful in detecting these autonomous vehicles, UAVs, UGVs, and outdoor robots (Dan et al. 2019; Fang et al. 2018; Krátký and Fuxa 2015; Vinogradov, Kovalev, and Pollin 2018a). High-speed railway network surveillance (Blázquez-García, Casamayón-Antón, and Burgos-García 2018), vehicle-to-vehicle (V2V) communications (Kwon et al. 2016) are some of the other applications that have considered deployment of LTE passive radars. However, a comprehensive survey considering the state-of-the-art in LTE-based passive radars has not been explored. Hence, this paper presents a comprehensive survey of LTE passive radars which have been considered in different application scenarios. Main focus of this survey article is to analyse the characteristics of the LTE signal structure that are helpful from the passive radar perspective. The key parameters of LTE passive radar along with the signal processing details are also discussed.

The remainder of the paper is organized as follows. In Section 2, introduction to passive radar is presented. LTE signal structure and overview details are given in Section 3. Key parameters of the LTE passive radars are presented in Section 4. LTE passive radar signal processing details are discussed in Section 5 in which various types of LTE passive radars are also presented. Section 6 introduces 5 G-NR radar research and future progress of LTE passive radar. Finally, Section 7 presents some concluding remarks.

2. Introduction to passive radar

A passive radar includes only a receiver without a paired transmitter. Passive radar has several advantages over active radar despite being having no transmitter, as no additional frequency bandwidth is required and which makes it invisible and unrecognizable to monitoring receivers and they also do not add additional interference. Further, the total system cost can be minimized as transmitter is not required in a passive radar system. In recent years, the deployment of the base station (base station provides the connection between mobile phones/users and the mobile network) for passive radar systems has attracted significant attention from the international radar community. Base stations like; Broadcast and terrestrial systems including FM radio station, 3 G GSM, and Digital Video Broadcasting (DVB-T) have been considered good contender for passive applications and have been practically implemented. This is primarily done for systems without any line of sight. The study of LTE signal and its structure for passive radar is a topic of current interest (Evers and Jackson 2014a; Raja Abdullah et al. 2015; Salah et al.

2013). LTE has well-defined cellular standards, which also expand the utilization of digital waveform for radars. LTE like GSM allows user equipment (UE) or receiver to synchronize with base station along with the processing of the received signal. In addition to these synchronization signals, features of LTE signal can be used to create good matched filters for range estimation and Doppler profile, which are the characteristics of any radar. This paper accumulates such radar characteristics and its use in the LTE cellular standard. Figure 1 gives an overview of the LTE-based passive radar.

2.1. Usage scenarios

The major applications of passive radars can be found in air, oceanic, and ground surveillance. The application area of passive radars depend upon base station properties. The most common and useful performance measures for inspecting the radar performance for a given signal/waveform are Range-Doppler (RD) map and an ambiguity function. Ambiguity function, in a broad sense, is used to analyse the waveform for passive radar utilization by investigating the Doppler and Range resolution (Evers and Jackson 2014a).

Some other applications of passive radar as shown in Figure 2 include industry automation (Xu et al. 2019), smart city surveillance (Gómez-del-Hoyo et al. 2015; Li et al. 2019), UGVs, UAVs/ Drones (De Quevedo et al. 2018; Jian, Lu, and Chen 2018; Liu et al. 2017), and smart parking (Sonny et al. 2020). In majority of these applications, it can be observed that passive radars using LTE are a favourable solution. Next, we present an overview of LTE physical downlink channel (DL) including its signal structure (3rd Generation Partnership Project 2010).

3. LTE signal structure & overview

LTE can use either of the two different transmission scheme: First one is frequency division duplexing also known as FDD and second one called as time division duplexing also

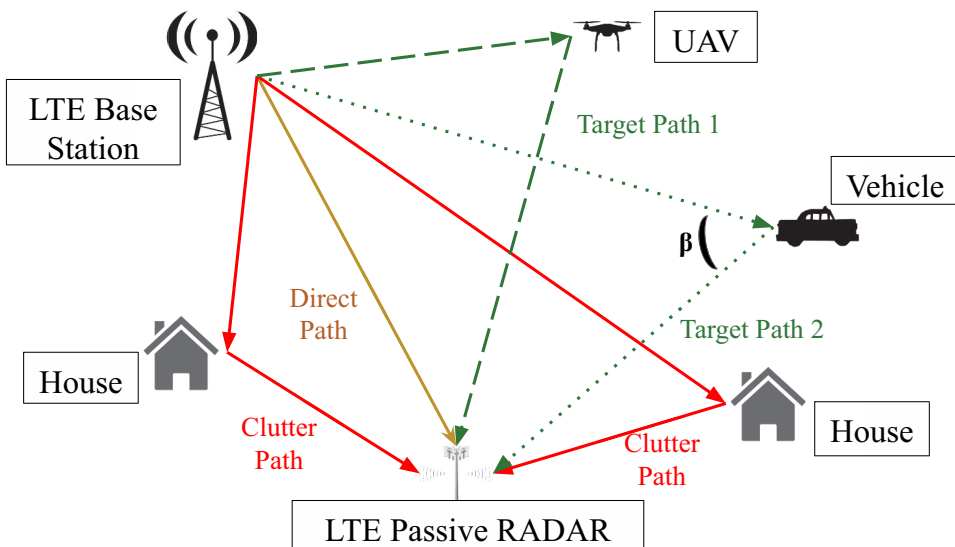


Figure 1. LTE passive radar for vehicles and UAVs.

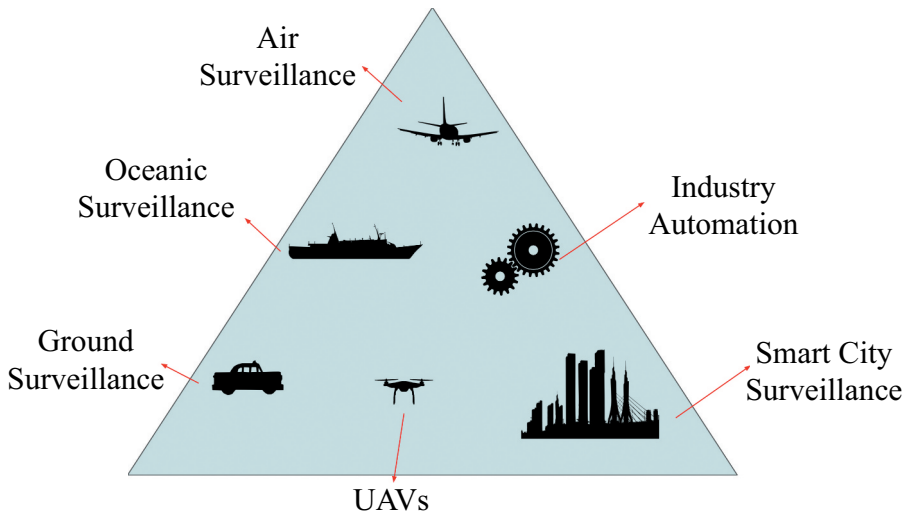


Figure 2. LTE passive radar usage scenario.

known as TDD. Both of these scheme use OFDM/OFDMA property. FDD has a different frequency band for both uplink (UL) and downlink (DL) transmissions, whereas, TDD serves both the uplink (UL) and downlink (DL) transmissions in same frequency band. For explanation of the signal details, we have considered only the FDD-DL in this paper as most of the Telecom service providers uses this transmission method. However, similar analysis is possible for the TDD-based LTE. The LTE standard considers various channel bandwidths like 1.4, 3, 10, 20 MHz. The channel bandwidth consists of P-subcarriers which have 15 KHz or 7.5 KHz separation frequency width support for LTE depending upon the configuration. The parameter, P, depends upon the number of FFT points considered.

Figure 3(a) illustrates the FDD LTE DL signal. The symbol is a collection of N orthogonal modulated sub-carriers, which also have guard band and Direct Current (DC) subcarriers as shown in **Figure 3(b)**. The typical sub-carriers contain the user data. These sub-carriers are modulated by either of the following modulation schemes: quadrature phase-shift keying (QPSK), 16 quadrature amplitude modulation (16 QAM), or 64 QAM. Then, the sub-carrier is sent to IDFT (inverse discrete Fourier transform) or commonly used inverse fast Fourier transform (IFFT) of the modulated signal. A cyclic prefix (CP) will be attached to this IDFT/IFFT sequence to reduce the multi-path effects. A cyclic prefix is a copy of small portion of the end part of IDFT/IFFT sequence, which is affixed at the start of IDFT/IFFT sequence. This complete sequence is known as a data symbol, which is also the basic generation method of an OFDM symbol. LTE has two cyclic prefix configurations as per standards; normal cyclic prefix or extended cyclic prefix (3rd Generation Partnership Project 2010). The normal cyclic prefix is preferably used when there is low delay spread channel, whereas, extended cyclic prefix is used when the channel has high delay spread. Normal cyclic prefix is used in most of the cases. A slot can either have $N_{SYM} = 6$ symbols for extended CP or $N_{SYM} = 7$ symbols for normal CP. FDD LTE DL data symbols have a slot duration of 0.5 ms, sub-frame of 1 ms, and a frame of 10 ms and this duration is constant throughout the transmission. The whole DL signal, consisting of one frame, can be used as a radar pulse. This was the basic overview of the FDD LTE downlink signal for radar

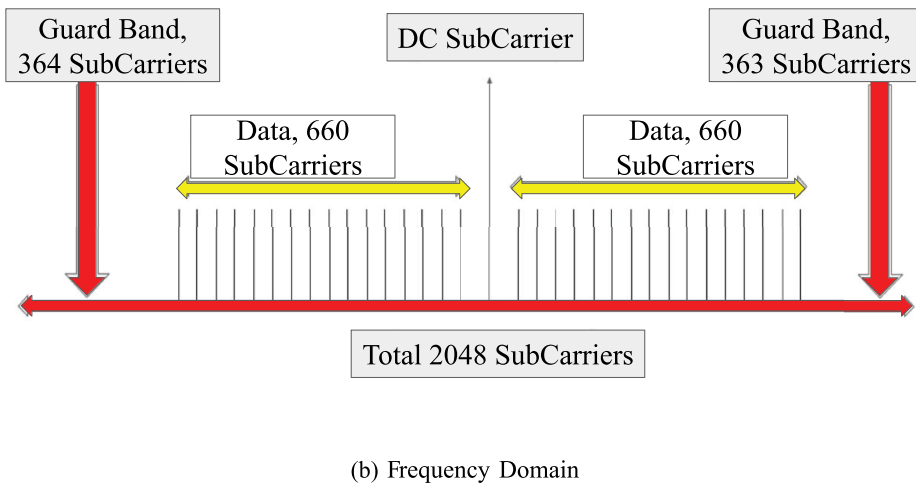
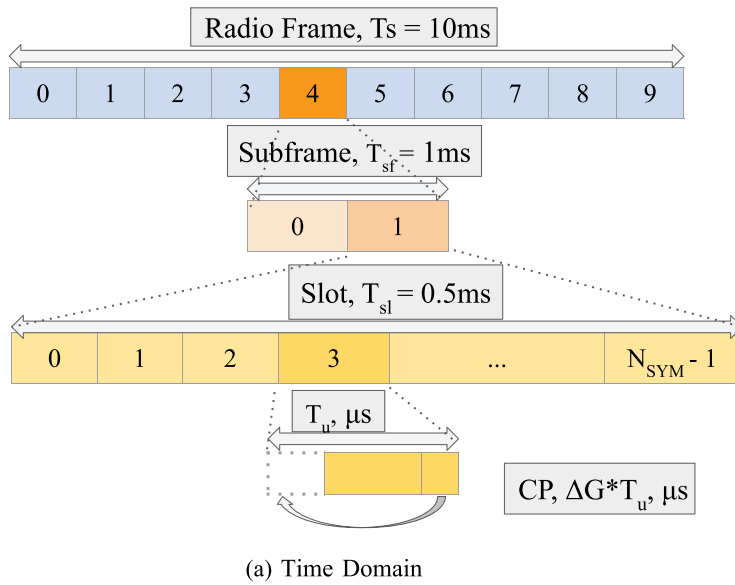


Figure 3. LTE downlink frame structure (3rd Generation Partnership Project 2010)

purpose. In the next part, cell-specific reference signals (CSRS) and synchronization signals (SS) are explained: which can be used for coherent radar processing.

3.1. Synchronization signals (PSS & SSS)

In LTE standard, there are two different synchronization signals for DL, which are used by receiver to get the cell identities (CIDs) and frame timings. The two different synchronization signals are: primary synchronization signal (PSS) and secondary synchronization signal (SSS). LTE base station have unique 504 physical layer cell identities (CIDs) for

a different cells so that a receiver or UE can segregate the information received from different base stations in vicinity of each other. These 504 CIDs are uniquely generated by the PSS and SSS. The PSS is made up of 62-length of Zadoff-Chu sequence. The output of these sequences are then mapped to sub-carriers of slots 0 and 10 of the last symbol. The details of the Zadoff-Chu sequence and others can be found in 3rd Generation Partnership Project (2010). For symbols carrying a PSS, the sequences are modulated and other sub-carriers are then modulated in which guard bands and DC sub-carrier are assigned as zero. Two binary sequences having length 31 are used to generate the SSS. These two sequences are scrambled making a total 62-length SSS. The mapping of SSS is done similar to PSS, SSS having length of 62 is mapped to 62 sub-carriers about the DC sub-carrier at centre. If first SSS signal is noticed at sub-frame 1, then the synchronization can be attained at the next frame having SSS signal in sub-frame 1. Cell search can be done by both PSS and SSS.

3.2. Cell Specific Reference Signals (CSRS)

Cell specific reference signals (CSRS) are deployed so that the UE/receiver can easily identify the transmitting antenna. The CSRS is generated by a pseudo-random Gold sequence having 31-length, the expression can be found in 3rd Generation Partnership Project (2010). This Gold sequence produces complex modulation values for each CSRS, which is modulated by quadrature phase shift keying (QPSK) modulation. Even though CSRS are complex as well as pseudo-random, it can easily be evaluated by the known physical layer CID. If Physical layer CID is not known, then using the PSS and SSS, it can easily perform the cell search and extract CID for CSRS (3rd Generation Partnership Project 2010).

The position of CSRS sub-carrier is determined by physical layer CID as well as number of antennas being used (3rd Generation Partnership Project 2010). For single antenna, the CSRS occupy symbols 0 and 3 in a slot where normal CP is being used. Whereas, for extended CP, CSRS occupy symbols 0 and 2 (note that this number can change with the number of antennas being used). The positions of the CSRS are given by the mathematical expression provided in 3rd Generation Partnership Project (2010). Further, CSRS are mapped on every six sub-carriers (shown in Figure 4), with consecutive CSRS symbol having a frequency offset of minimum three sub-carriers. Figure 5 gives a graphical indication of an example for the location of CSRS.

Figure 6 shows a measured LTE down-link transmission using universal software radio peripheral (USRP) E312 from Ettus for a centre frequency of 1.83 GHz (Telenor operator). Unlike conventional broadcast signals, LTE physical down-link signals barely exist at every time instant to lower the power consumption (of both UE & base station). Figure 4 shows the resource grid of collected LTE waveforms, which also shows random and deterministic components in real-time LTE. The deterministic components are the important ones for down-link processing, which include: secondary synchronization signal (SSS), primary synchronization signal (PSS), cell specific reference signal (CSRS), physical down-link shared channel (PDSCH), physical broadcast channel (PBCH), and physical down-link control channel (PDCCH). During the idle state of base station or evolved Node Base (eNB), the UE receives only noise. A detailed description & explanation of the down-link and up-link signals and deterministic channels can be found in 3rd Generation

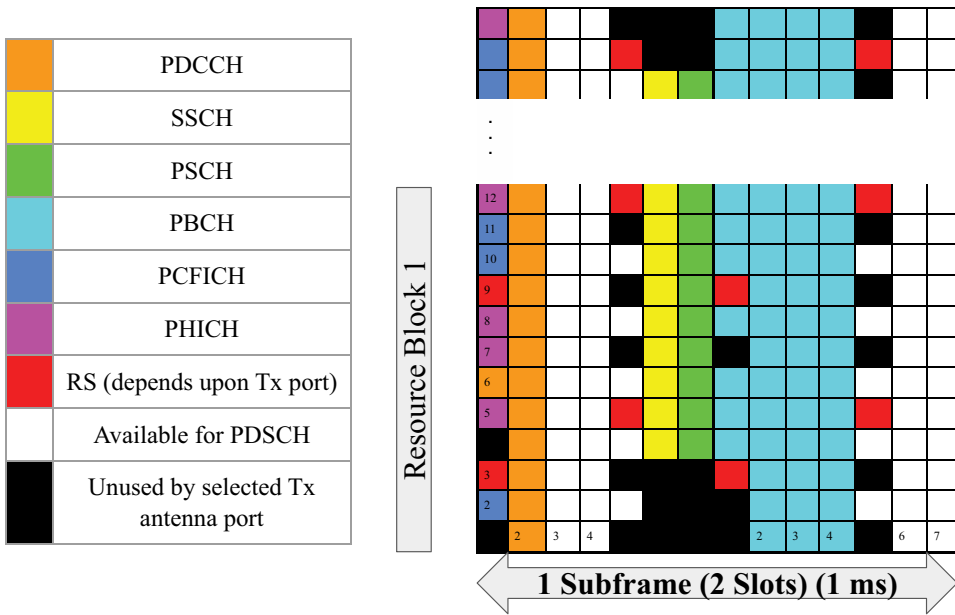


Figure 4. LTE FDD resource grid (3rd Generation Partnership Project 2010)

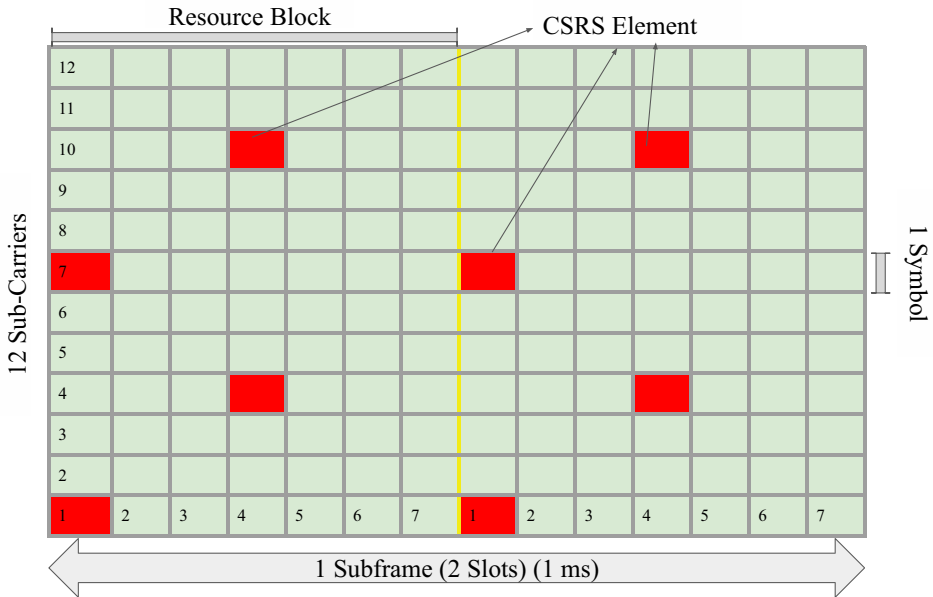


Figure 5.. Time-frequency grid of a CSRS.

Partnership Project (2010). Next, we discuss suitable parameters to be considered for a passive radar system.

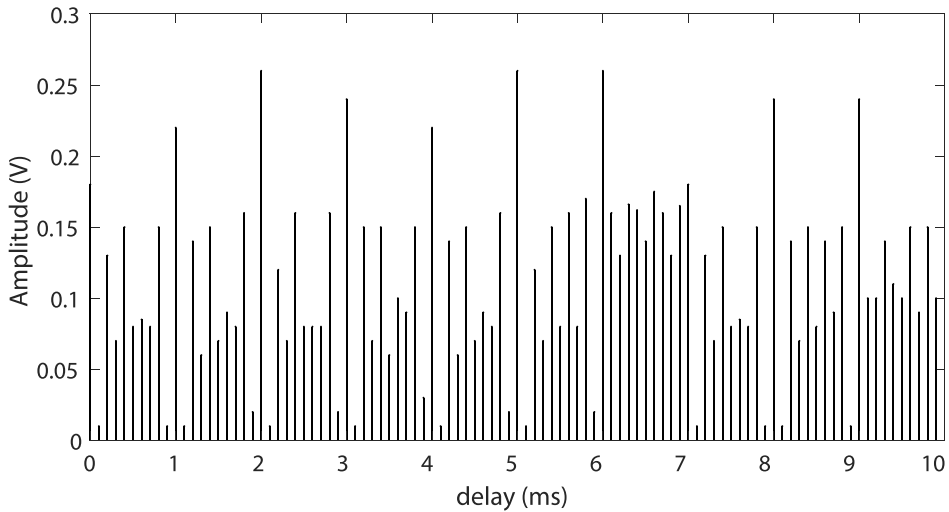


Figure 6. LTE real-time waveform.

4. Passive radar parameters

In this section, we discuss the key passive radar parameters, namely, ambiguity function, range/velocity resolution, and range-doppler map.

4.1. Ambiguity function

The ambiguity function (AF) or commonly known as cross ambiguity function (CAF) is done between two different signals to show the properties of the radar waveform, which include resolution (range, angle) and ambiguities Doppler dimension as well as ambiguities in delay (Costas 1984). The AF is defined as

$$\tilde{\chi}(\tau, f_D) = \int_{-\infty}^{\infty} x(t)x^*(t - \tau)\exp(j2\pi f_D t)dt, \quad (1)$$

where, $x(t)$ represents the transmitted signal or waveform, $*$ denotes the complex conjugate of signal, τ denotes delay and f_D denotes Doppler shift. The τ can also be defined as the radial delay with respect to the receiver. Bi-static radar is a type of radar consisting of a transmitter and receiver separated by some distance. Figure 1 represents the passive bi-static radar in which transmitter location is unknown to receiver and they are separated by some distance. For the bi-static radar, bi-static delay should be considered, which is the ratio of the bi-static range and the speed of light.

Figure 7 depicts the typical AF of a real-time LTE signal. It actually shows the relation of delay, Doppler shift, and intensity of reflection (which is proportional to target cross section) from target. The following purposes are served by the CAF. It provides the necessary gain for signal processing to detect targets (matched filter). It is used for estimating Doppler shifts and target range. If any target is detected, a spot will be made in graph with respect to target cross-section (intensity) of the target and the τ delay.

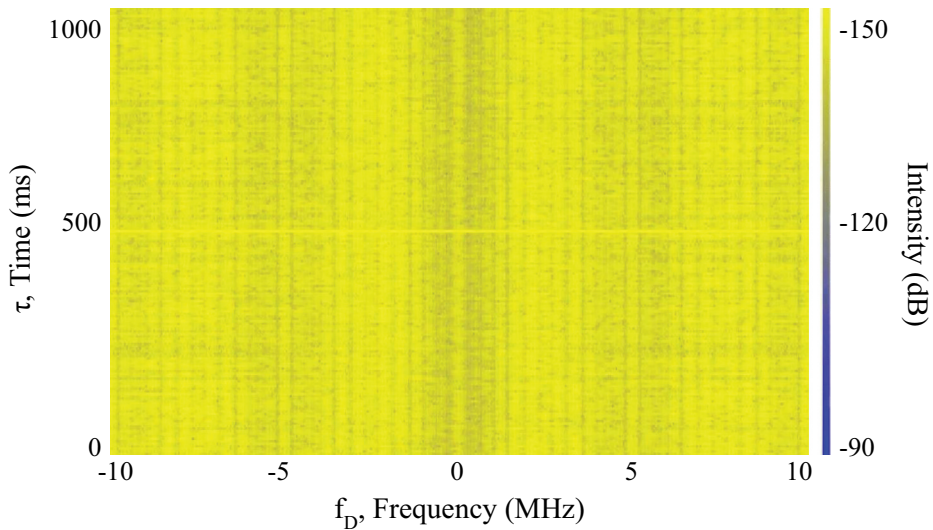


Figure 7. Ambiguity function of real-time LTE signal.

4.2. Range and velocity resolution

Range resolution, ΔR is the minimum distance required by the radar to differentiate two different targets, which can either be moving with the same or different velocities and having bi-static bisector (β) between the transmitter-target-receiver as shown in [Figure 1](#). It is given as (Salah et al. 2013; Raja Abdullah et al. 2015)

$$\Delta R = \frac{c}{2 * BW * \cos(\beta/2)}, \quad (2)$$

where, BW is bandwidth of the transmitted signal, c represents the speed of light (3×10^8 m/s), and β is the bi-static angle between the transmitter-target-receiver. The standard LTE signal bandwidth varies from 1.4 MHz to 20 MHz depending upon the location and telecom operator. Thus, the range resolution can vary from 8.66 m to 34.6 m with the LTE bandwidth of 20 MHz to 5 MHz, assuming the conventional bi-static angle to compare with existing passive bi-static radar like FM/GSM to be $\beta = 60^\circ$ as shown in Tan et al. (2005b). [Table 1](#) and [2](#) highlights some key differences in these technologies in terms of there signals.

The Doppler resolution is used to differentiate the targets moving at various velocities or a single target moving with the different velocities. This Doppler resolution can be calculated from the CIT (coherent integration time) of the receiver. It is given as

$$\Delta f_D = \frac{1}{T}, \quad (3)$$

where, T is the coherent integration time and Δf_D is the Doppler shift/resolution. The velocity resolution can be defined as the ability of radar to differentiate at least two targets moving in different velocities at the same range. It is defined as

$$\Delta v = \frac{\lambda}{2 * T * \cos(\beta/2)}, \quad (4)$$

where, λ represents wavelength, Δv represents velocity resolution. Considering T to be 0.5 sec, we will have $\Delta f_D = 2$ Hz, and with $\lambda = 0.16$ m, $\beta = 60^\circ$, we will get velocity resolution Δv of 0.189 m/s. Hence, LTE passive radar can differentiate two targets moving at a velocity difference of 0.189 m/s.

4.3. Range-Doppler map

From a Range-Doppler map, we can see how far the targets are and their movements. It differentiates among the targets moving with different velocities at different ranges. For example, for a stationary transmitter, a Range-Doppler map shows an output for the stationary targets/objects at zero Doppler. In case the targets are moving for a stationary transmitter, the Range-Doppler map will show a response at non-zero Doppler values which can be observed in Figure 8. We can also use the Range-Doppler response in other ways, for e.g. to extract peak information/detection in the Range-Doppler map and use that information for classification, etc. The standard signal processing uses RD (Range-Doppler) map which is directly related to 2-Dimensional CAF. An example of Range-Doppler Map is shown in Figure 8. Further, for detection of small targets, we need to compute higher order of FFTs (2D/3D FFT) (Petri et al. 2012). Next, we present some basics of radar signal processing.

5. Radar processing

To extract the range and velocity of the target, the received signals are processed as shown in Figure 9, which provides the overall processing flow of typical passive radar. At the receiver, we get the received signal $x(t)$ that consists of direct path signal, Doppler echoes occurred from device noise, and the target signal. It can also be shown mathematically as

$$x(t) = \alpha x_e(t - \bar{t}) + \sum_i \epsilon_i x_e(t - \tau_i - \bar{t}) + \sum_j \gamma_j x_e(t - \tau_j - \bar{t}) \exp(j2\pi f_D t) + \eta(t) \quad (5)$$

where,

- \bar{t} is the signal delay between the transmitter and the receiver,
- $\tau_j + \bar{t}$ and $\tau_i + \bar{t}$ are the delays between the receiver and the j^{th} target and the respective i^{th} static reflector (from environment like tree, house),
- f_D is incurred due to the motion of target also known as frequency shift (due to Doppler effect),
- α , ϵ_i , γ_j are complex attenuation factors. γ_j and ϵ_i are, respectively, RCS (radar/receiver cross-section) of the various reflectors and positions, and
- $\eta(t)$ is the device noise which is typically Gaussian in nature.

The transmitted signal, x_e is not precisely known. This signal is said to be a reference signal denoted by $x_{\text{ref}}(t)$ which we consider to be calculated by LOS/direct path signal. Then, the (5) can be rewritten as:

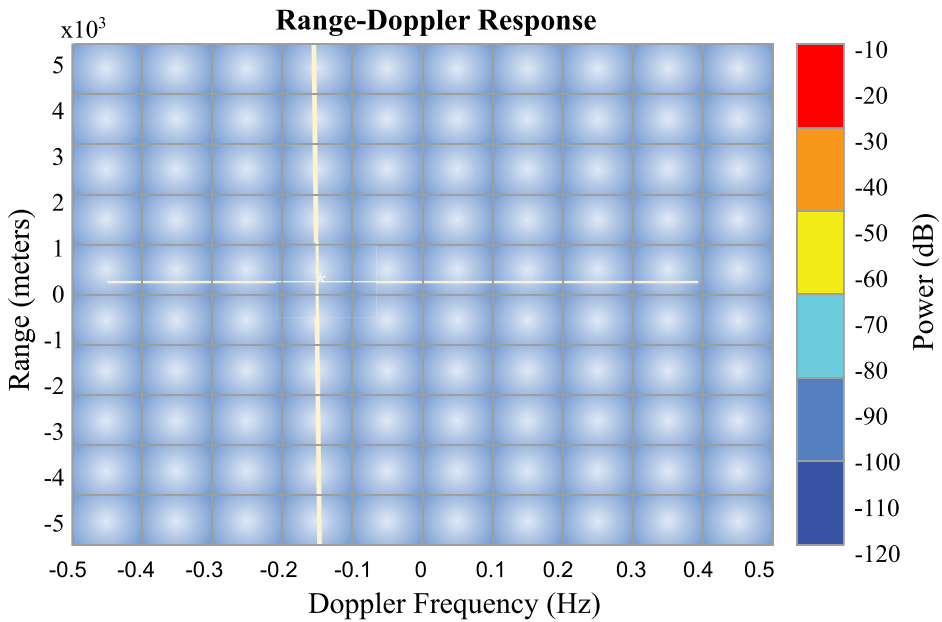


Figure 8. An example of Range-Doppler map.

$$x(t) = \alpha x_{\text{ref}}(t) + \sum_i \epsilon_i x_{\text{ref}}(t - \tau_i) + \sum_j \gamma_j x_{\text{ref}}(t - \tau_j) \exp(j2\pi f_D t) + \eta(t). \quad (6)$$

Typically, the target's RCS is small, hence γ_j is very small compared to $|\alpha|$ and $|\epsilon_i|$.

It is therefore important to amplify the target signal from the $x(t)$, the received target's echoes denoted as

$$x_{\text{tar}}(t) = \sum_j \gamma_j x_{\text{ref}}(t - \tau_j) \exp(j2\pi f_D t). \quad (7)$$

To remove the unnecessary reflections, which is a clutter from clutter path denoted as

$$x_{\text{clut}}(t) = \alpha x_{\text{ref}}(t) + \sum_i \epsilon_i x_{\text{ref}}(t - \tau_i). \quad (8)$$

Finally, the reference signal $x_{\text{ref}}(t)$, is compared or correlated to the 'clutter removed' processed signal $x_{\text{clut}}(t)$ to estimate the range and velocity of the target.

5.1. Recovery of the reference signal

The LTE contains pilot signals which at the time of cross ambiguity function calculation give deterministic peak that spread over the range Doppler map. Figure 7 shows the ambiguity function of a real-time LTE signal. The pilot signals have generated the peaks which can be clearly seen at non-zero Doppler shifts. This complicates the target detection and thus can cause false alarms. Hence, from the target path signal, the direct path signal has to be suppressed. Figure 9 depicts the typical passive radar processing. To do

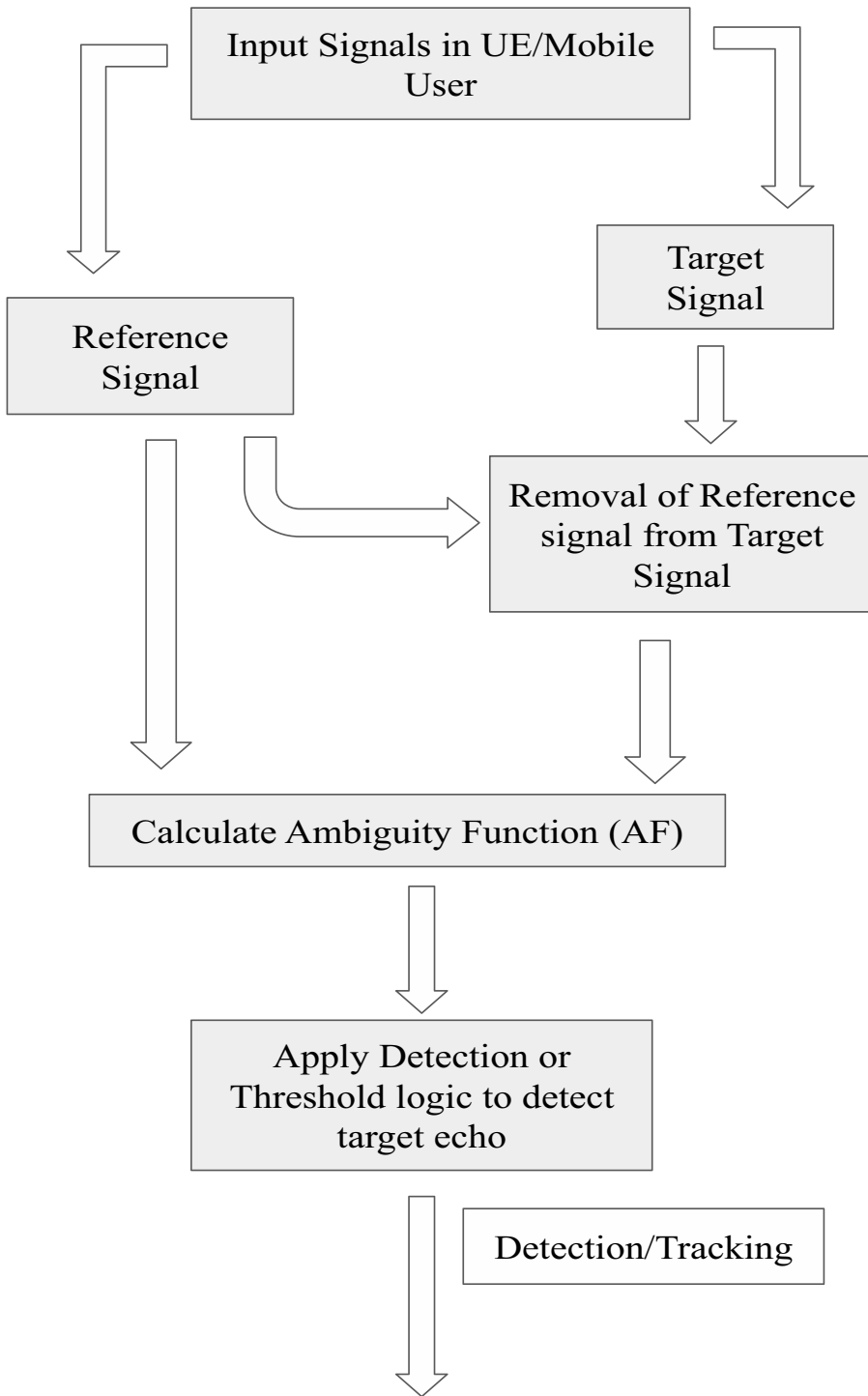


Figure 9. LTE passive radar processing.

this, a good duplication of reference signal has to be acquired from the surveillance antenna/port route. Recovery of reference signal of LTE consists of the following steps.

- (i). A time synchronization like PSS & SSS is executed to detect the start of LTE OFDM symbol. (ii). Frequency synchronization is executed to arrange sub-carriers with their respective FFT bins which also includes removal of cyclic prefix from OFDM symbol. (iii). Pilot sub-carriers like CSRS or any LTE reference signal (Note: Here the reference signal means the standard LTE Reference signal like CSRS, DMRS, etc.) symbols are used for channel equalization. (iv). Once channel equalization is done, the whole procedure is then carried out in the reverse direction to get a good reference signal.

5.2. Estimation of the propagation channel

This step is commonly used for active radar systems. To simplify, we are considering a noiseless case without reflections from moving targets. Then the received signal contains only the direct path and static-object reflected signal. But the noise $\eta(\mathbf{t})$ and Doppler reflections $\mathbf{x}_{\text{tar}}(\mathbf{t})$ exist in the system which create error on the estimation. However, at the weak Doppler reflections and at adequate signal-to-noise ratio (SNR), mapping of estimated data allows it to correct most of the errors, i.e. data can be perfectly recovered. Hence, if we can perfectly recover the data then the channel estimation can easily be performed and vice-versa, with various available channel estimation algorithms Shao Min and Nikias (1994).

5.3. Target detection technique

For the target detection, a threshold value is set on the output of the CAF. The threshold is adapted according to the noise floor variance for given false alarm probability (P_{fa}). Detectors like cell averaging constant false-alarm rate (CA-CFAR) are available in the existing radar literature Richard (2014). An example of CA-CFAR is to use Doppler shift and delay points in the CAF corresponding to a cell. A threshold around the cell under test (CUT) can be set from the level of noise floor variance. It is done by calculating the average power level of the different cell blocks about the CUT. Target signal returns spread across multiple cells. A target can be termed 'captured' in the CUT only if the CAF of that specific cell is larger than the adjoining cells and with respect to the average power level. This process is run on the full CAF map.

5.4. Different types of LTE passive radars

The CAF presented in earlier sections is computed between the filtered target signals and reformed reference signal to evaluate the Doppler shifts & range of the target,

$$|\tilde{\chi}(\tau, f_D)| = \left| \left(\int_{-\infty}^{\infty} x_{\text{ref}}(t) x_{\text{tar}}^*(t - \tau) \exp(j2\pi f_D t) dt \right) \right|, \quad (9)$$

where, $x_{\text{ref}}(t)$ is the reformed reference signal, $x_{\text{tar}}(t)$ is the filtered surveillance/target signal, τ is the time delay which is occurred due to signal reflection from the target, and Doppler shift/frequency shift is represented by f_D . Various types of AF can be used for LTE

passive radars and different LTE passive radar techniques available for target detection (Evers and Jackson (2014a; 2014b) are summarized in the next section.

5.4.1. LTE DL self ambiguity function

Considering $x(t)$ to be one radio frame on down-link transmission, the matched filtering is performed on it as a received radar pulse. Figure 10 is the output plot of (9) for the self-ambiguity function (SAF) case, $x_{\text{ref}}(t) = x(t)$. In Evers and Jackson (2014b), it has been shown that the SAF of LTE DL signal for one radio frame will have two peaks at notable locations: The first one at zero delay and the second peak at the zero Doppler. The presence of CP portion in the symbol causes the generation of secondary peak as discussed in Section 3. Similarly, these kind of outcomes from the PSS, SSS, and CSRSs are expected as they also produce AF peaks, which are further discussed in the following section.

In Figure 10, first peak is present at zero-Doppler and second peak is due to the cyclic prefix (CP) and is located at T_u time instant. Based on the peak locations in Figure 10, the radar range for the mono-static case (the system in which transmitter and receiver are collocated) is $cT_u/2 \approx 10$ km. From Table 1, 5 MHz LTE DL signal bandwidth will have a range resolution of ≈ 34 m. Hence, range bins, which is the ratio of radar range and range resolution will be around 333. From Table 1, we have carrier centre frequency to be 1850 MHz and CIT to be 10 ms which gives velocity resolution of ≈ 20.59 m/s. This velocity resolution is different from the velocity resolution discussed in Section 4.2. Here, only one radio frame is considered, whereas, in Section 4.2, the whole LTE radio frame is considered.

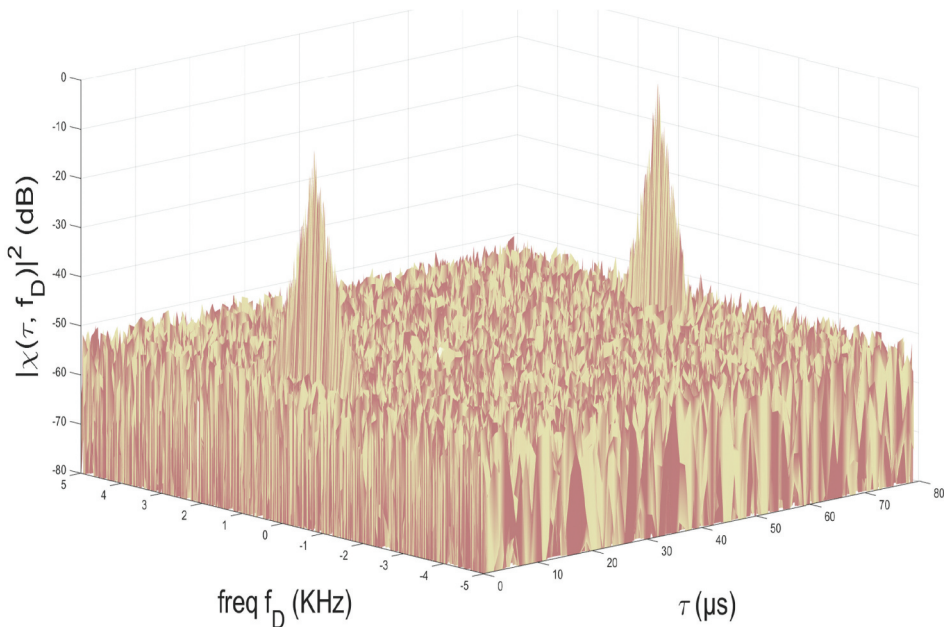


Figure 10. SAF of an LTE DL signal.

Table 1. LTE signal parameters in UiA NORWAY for TELENOR operator.

PARAMETERS	SYMBOL	VALUE
Carrier frequency (GHz)	f_c	1.83
EARFC Number		1450
Physical Cell Id	PCI	123
Bandwidth (MHz)	B or BW	5
Subcarrier Separation (KHz)	Δf	15
Data Subcarriers	N_A	1200
Subcarriers Per Symbol	N	2048
Data Symbol Duration (μ s)	T_u	66.7
Cyclic Prefix Ratio	ΔG	1/4
Symbol Duration (ms)	T_{SYM}	8.5
Symbols	N_{SYM}	25
Signal Duration (ms)	T_S	196.3
Modulation Scheme		64 QAM

Table 2. Different signal source for passive radar with its waveform properties.

Base station	Center frequency (MHz)	Band width (KHz)	Range resolution (m)	Velocity resolution (m/s)
GSM	940	81.3	1845	0.33
DVB-T	505	6000	25	0.61
FM	97.3	50	3000	3.29
WiFi	2434	20,000	7.5	0.13
WiMAX	2110	20,000	7.5	0.15
LTE – Band 3	1830	5000	34	0.189
LTE – Band 7	2635	20,000	7.5	0.11
LTE – Band 28	728	20,000	7.5	0.3
LTE – Band 3 (CSRS & SS)	1830	5000	28–34	20.59
5 G-NR	60,000	50,000	0.5–3	1

Since the received signal contains ‘user’ data which is not known, it is computationally expensive to build and perform the matched filtering. Hence, a direct path signal is needed, and in addition the received signal has to be decoded which requires a prior information to create an ideal reference signal. Hence, in Section 5.4.3 and 5.4.4, we consider a prior reference and known signals for radar response so that a matched filter could be designed and filtering can be done in simpler manner for LTE DL signal as in 3rd Generation Partnership Project (2010).

5.4.2. CP OFDM based concept

Inter symbol interference (ISI) is a common problem in wireless communication channel, one symbol may overlap with the adjacent symbol due to the delay spread in the channel. To combat this ISI, 3rd generation partnership project (3GPP) has proposed/established a guard period for LTE signal. Figure 3(a) shows the guard period/interval which is essentially the cyclic prefix (CP) 3, i.e. some end portion of that symbol is prefixed to that same symbol. It means that LTE passive radar could follow the radar processing from CP-OFDM pattern Berger et al. (2008), (2010); Chabriel et al. (2014); Wan et al. (2014); Xiaoqi Yang et al. (2016). As shown in Figure 1, surveillance antenna receives reflected echo from UAV (Direct Path 1, 2), echoes from clutter path (house, tree) and from the direct path as well. If the clutter path possesses high energy, then at CAF, the UAV might be undetectable due to the side-lobes created by the clutter path. This situation generally happens when there is tall, dense infrastructure, buildings, and obstacles are present in

environment around the base station. So, in the surveillance channel, one should carefully use the direct path signal and multi-path clutters. To overcome, multi-path effects and to recover the data, the structure of CP-OFDM signal provides a low complexity solution. Hence, we can actually apply the channel estimation technique which lacks in other passive radars. The processing steps for CP-OFDM are as follows.

Data can be recovered by an estimated channel. This data is then used to analyse the original signal, which further is used as a reference signal for CAF. It is then possible to analyse the wireless channel of the clutter path (reflections from reflectors like tree, house, also includes direct path), to remove the clutter signal.

Clutter Removal for CP-OFDM: This method assumes that over the symbol, the clutter effect is same. We have already seen if the original data can be recovered, it is also possible to estimate, and synthesize the clutter. In Chabriel et al. (2014), a frequency clutter removal method has been presented which is broadly explained in Figure 11. The clutter can easily be removed to obtain the target reflections from the surveillance channel.

Once clutter is removed, RD Map can be produced by applying matched filtering technique on the target and reference signal, which is 2D discrete Fourier transform (DFT). Then, we can get information of bi-static range and velocity. However, there exist challenges associated with this method, radar receives noise and multi-path signal of down-link physical channels (DPCs) at the ideal state of base station (eNB), i.e. the state at which UEs is not in touch with base station to save energy. Hence, this problem has to identified as it will affect the matched filtering and clutter cancellation performance.

In Dan et al. (2019), an LTE Passive radar for UAV detection using an SDR has been proposed. A bandwidth of 15 MHz for a 10 m range resolution has been considered in Dan et al. (2019). In the receiver system, 18 dBi gain 18-elements Yagi-uda antenna with 32° beam-width in both the reference and target antennas have been used in SDR Krátký and Fuxa (2015); Vinogradov, Kovalev, and Pollin (2018b). In this, CP OFDM-based passive radar concept has been used. The UAVs maximum velocity equal to 20 m/s, LTE centre frequency of 2 GHz, and a 250 Hz as the maximum Doppler frequency for moving target (UAVs) has been considered. The developed radar system suits the low-altitude traffic monitoring.

5.4.3. CSRS cross ambiguity function

In CSRS CAF, $x_{ref}(t)$, is made-up of using $x_{CSRS}(t)$, which contains only the CSRSs (and rest of the symbols and sub-carriers are zeroes). From Section 3.2, it is already seen that the CSRSs occupy every third/fourth symbol of every sixth sub-carrier (depending upon antenna configuration 3rd Generation Partnership Project (2010)), with successive CSRS symbol having a three sub-carrier frequency difference. According to Levanon and Mozeson (2004), the CAF for a pulse frequency train is depicted in Figure 12 and given by

$$|\tilde{\chi}(\tau, \nu)| = |\tilde{\chi}_{Q=1}(\tau, \nu + k_s \tau)| * \left| \left(\frac{\sin(Q\pi(\nu + k_s \tau))}{Q \sin(\pi(\nu + k_s \tau) T_p)} \right) \right|, \quad (10)$$

where, signal ambiguity output for one period is $\tilde{\chi}_{Q=1}(\tau, \nu + k_s \tau)$, T_p is the PRI (pulse repetition interval) of the signal, and k_s is the frequency slope.

The frequency slope of CSRS signals is given by

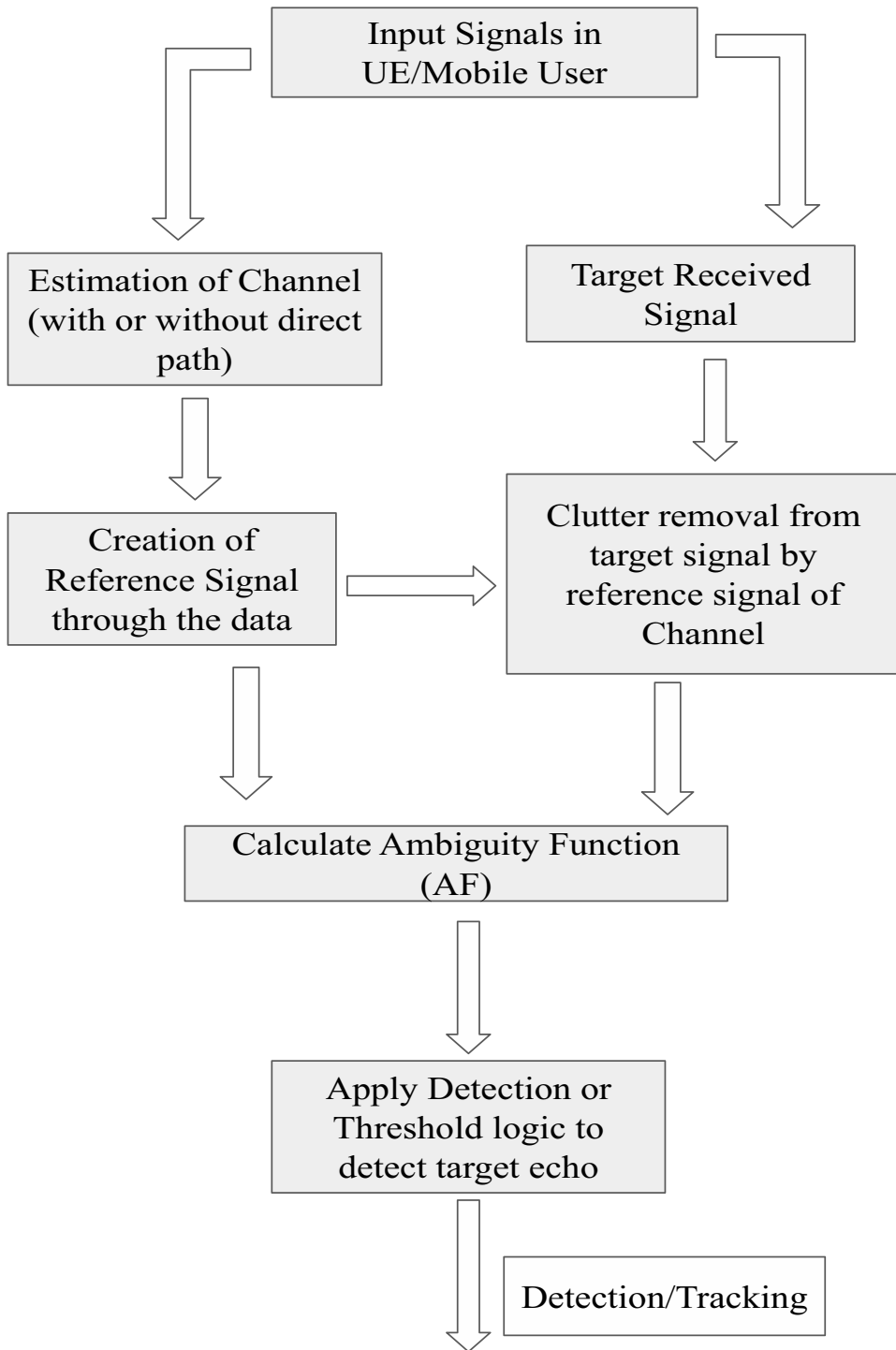


Figure 11. CP-OFDM based detection.

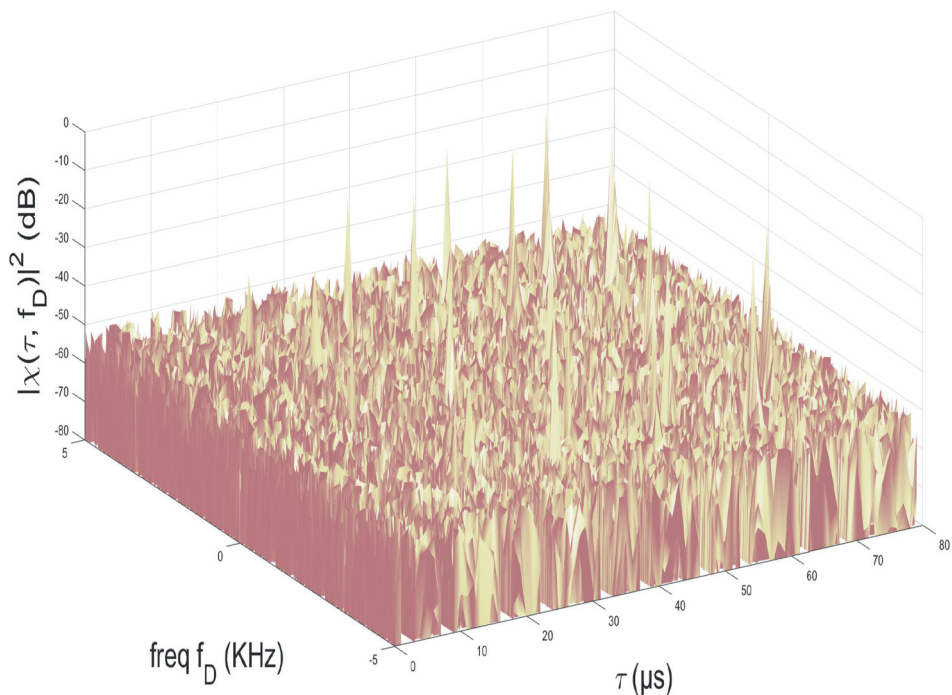


Figure 12. CAF of an LTE CSRS signal.

$$k_s = \pm \frac{3\Delta f}{3T_{\text{SYM}}}, \quad (11)$$

The resulting peaks locations of the CSRS CAF are given by

$$\begin{aligned} (\tau', \nu') &= \left(\frac{n_\tau T_u}{6} + 6zT_{\text{sym}}, \frac{n_\nu}{3T_{\text{sym}}} + \frac{n_\tau}{6T_{\text{sym}}} + 6\Delta fz \right) \\ &= ((11.11n_\tau + 500z)\mu\text{s}, (4n_\nu + 2n_\tau + 90z)\text{KHz}), \end{aligned} \quad (12)$$

where, n_τ , z , and n_ν are integers. The total energy contained in $x(t)$ will be more than $x_{\text{CSRS}}(t)$.

The knowledge of CSRS allows to generate the reference signal for the radar. There is no change in range resolution (≈ 30 m) as compared to the full LTE DL signal. But velocity resolution is changed (≈ 21 m/s) slightly.

Despite having many similarities, $x_{\text{CSRS}}(t)$ is not as powerful as $x(t)$. As shown in Figure 10 & Figure 12, the difference of maximum value of the CSRS-CAF and maximum value of the DL-SAF is -12.55 dB. Hence, this method will work for vehicle detection when matched filtering is done with the CSRS signal for a higher signal to noise ratio (SNR). Although $x_{\text{CSRS}}(t)$ does not provide good performance as compared to $x(t)$, i.e. LTE DL, it certainly offers a cost effective approach, which requires simple processing technique and less hardware for some applications.

5.4.4. Synchronization signals CAFs

Similar to the approaches presented in the previous subsections, a matched filter based on the information of synchronization signals (SS) features so that $x_{\text{ref}}(t) = x_{\text{SS}}(t)$ is considered here. A sub-frame is divided into slots of 14 successive symbols, the slots have a duration in milli-seconds which depends on adjustment of symbol timings. It can be calculated by detecting the synchronization signal (PSS & SSS). The range estimation can be done by time-domain PSS correlator. The PSS is 63-length m-sequence in frequency domain (including DC subcarrier), and the PSS eases frequency and time ambiguity offset from Zadoff Chu sequence of 62-length for LTE. The CAF of PSS & SSS is shown in Figure 13. The zero Doppler peak occurs due to CP at $T_u = 66.67 \mu\text{s}$ and the non-zero peaks are from the auto-correlation sequences of Zadoff Chu and binary sequences, which define the synchronization signals (SSs) and the reason of largest peak occurred outside the zero delay 3rd Generation Partnership Project (2010). However, the synchronization signals large pulse repetition interval (PRI), results in peaks in every $166 * T_{\text{SYM}} \approx 182 \text{ Hz}$ along the zero delay, from the Dirichlet sinc term Evers and Jackson (2014a). Further, the Sync signals occupy only 62 sub-carriers (for 20 MHz) in the middle of LTE DL signal bandwidth, which degrades the range resolution to $\approx 40\text{--}50 \text{ m}$. Similar to the signals, the SS provides the velocity resolution of $\approx 21 \text{ m/s}$. Even-though the capabilities of $x_{\text{SS}}(t)$ is limited to $x(t)$ like CSRS, the synchronization signals also offers simpler processing.

5.4.5. MIMO in LTE

LTE employs MIMO technology to enhance data rate and reliability. In case transmit diversity is used, similar content is transmitted or broadcasted on the resource grid from multiple antennas, making their CAF or AF similar. Hence, the total CAF or AF remains unchanged. Let us consider a MIMO systems consisting of M transmit and N receive antennas. We assume the signals which are being transmitted from the different antennas are non-overlapping on same bandwidth, and each receiver has N-element array. The signal at the N^{th} receiver of i^{th} element is the sum of target path, direct path,

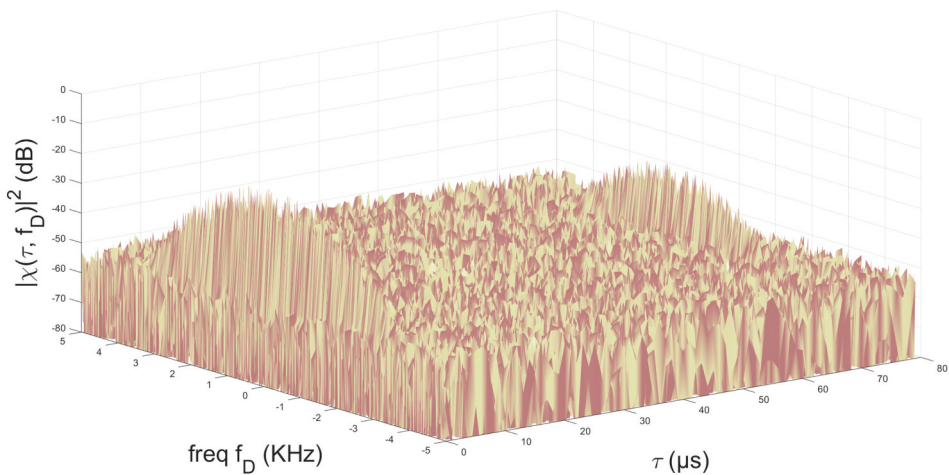


Figure 13. CAF of an LTE SS signal.

and clutter signals from each of the M transmit antennas. Figure 14 shows the conventional LTE MIMO passive radar.

A MIMO radar system prototype can be classified in three groups Fishler et al. (2004):

- Conventional radar array: This system consists of a transmitter array and a receiver array. The elements of array are separated by half wavelength distance to allow beam-forming and direction finding (DF).

- MIMO radar for DF: In this system, antennas at the transmitter are spaced widely to support targets spatial diversity property and array in receiver performs DF. This scenario has been addressed in Khawar, Abdel-Hadi, and Clancy (2014). The respective pairs of antennas are sufficiently separated to meet the orthogonality condition ($d = \lambda/2$) for targets of interest. Some common aspects:

- Assuming the antenna elements of both the transmitting and the receiving sides are omnidirectional.

- For processing, multiple independent copies of the received signal are available.

- When the number of receiving antennas exceeds the number of transmitting antennas, the channel parameters are known (Multiple orthogonal copies of the same signal).

- This will eventually increase the diversity gain and degree of freedom.

- Multiple target detection: In this system, MIMO radar is used to detect multiple objects/targets. In this, transmit antennas are less separated than in the previous scenario, such that the scatters belonging to the same target are resolved. The detection technique will be similar to Direction Finding, with the exception that the entries on the receiving correlation matrix will be completely uncorrelated due to the non-orthogonality of the received signal reflected by multiple targets.

MIMO radar can also be considered as a special case of many traditional radars. Further, with M transmit and N receive antennas, the channel response matrix can be considered as a space-time channel response density matrix which is function of space and time. Several channel estimation are available for the MIMO LTE scenario such as least squares

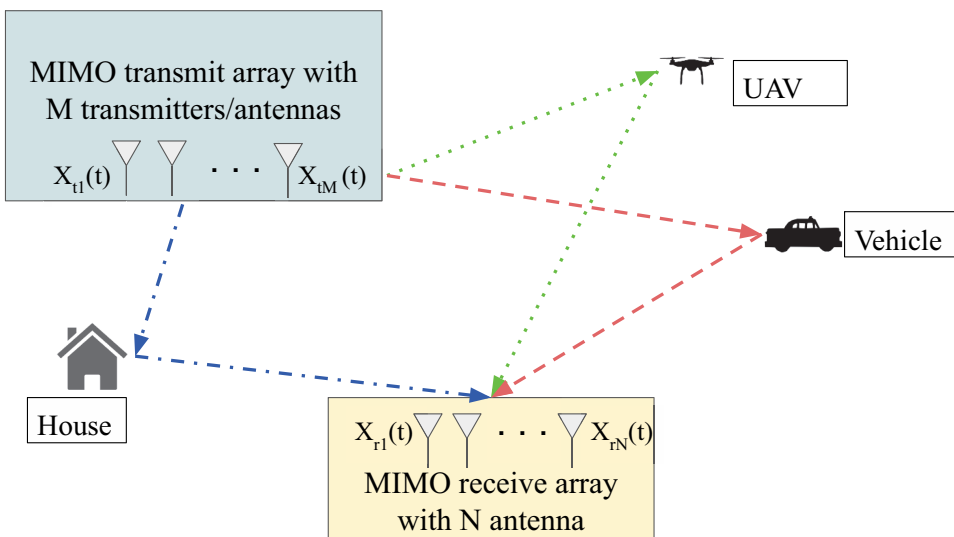


Figure 14. Conventional LTE MIMO passive radar.

or minimum mean square estimator (MMSE) Gesbert et al. (2003); Wubben et al. (2003). On the other hand, Colocated MIMO radars have antennas that are close together and see the targets from the same angle. One of the primary benefits of colocated MIMO radars is their high angular resolution due to waveform diversity Haisheng et al. (2015a), Haisheng et al. (2015b).

In Bliss and Forsythe (2003), the performance of two MIMO and one classical array system has been compared. It has been shown that the MIMO improves resolution compared to traditional radar systems. There exists many detectors like Gram matrices (PSL-GLRT, PMR-GLRT) and non-coherent integrator (like AC-CAF, C-CAF, AMR-GLRT, D-CAF) Hack (2013) which employs detection fusion integration (M-of-N) for MIMO scenario.

The key topics that can be summarized for MIMO radar are as follows.

- Targets with a diverse back-scatter, perfect processing of LTE MIMO radar leads to increase in diversity gains in the form of improved signal-to-noise ratio (SNR). The energy collected from the scatterers reflection is being processed and combined non-coherently.
- MIMO radar can detect and resolve targets which are closely spaced with high resolution.
- A good diversity gain for DF can be achieved with MIMO radar which have a transmitter and receiver array which are widely distributed.
- Targets moving in different directions can also be observed over an angular sector.

Main advantages of MIMO radar are:

- Direction finding, Static or moving target detection, Diversity gain, MIMO radar can use adaptive detection techniques, and Multidimensional space for processing can be done with the use of spatial multiplexing in MIMO configuration by the combination of transmit and receive antennas.

In Khawar, Abdel-Hadi, and Clancy (2014), the concept of MIMO LTE radar spectrum sharing between a LTE configuration system and MIMO radar with several base stations in different cells has been considered. Since a cellular system has several base stations, it will give rise to more than one interference channel which can again be used for radar processing.

5.4.6. LTE Commensal Radar

LTE Commensal Radar is a novel way to use existing LTE infrastructure to monitor environmental changes and assess feasibility. Santu et al. named the system LTE-CommSense, and it can be used for a variety of environmental sensing objectives such as disaster monitoring, sea state monitoring, snow avalanche monitoring, security of large unmanned landscapes, and so on. This technology focuses on known reference symbols in LTE signal frames, which are used to estimate changes in channel properties. LTE spectrum will be used to obtain channel estimates without interfering with existing infrastructure, allowing it to be used as passive radar.

This method senses the environment and predict/classify the objects. This method is useful for both indoor and outdoor scenario where the field of interest is small, i.e. 20 m as well as in indoor localization (Sardar et al. 2018b). In Sardar, Mishra, and Khan (2017, 2018a, 2020) a new method, CommSense, which uses LTE telecom infrastructure to sense the environment change has been proposed. It is a receive-only system. It checks and differentiate the received signal with the expected reference signal to detect the changes

in the channel environment. After the channel estimation process, application-specific instrumentation (ASIN) framework is used to detect the environmental change as shown in Figure 15. The data is taken with the help of USRP-SDR but any device can be used in which LTE signal is captured. The channel estimation block output contains information like fading, scattering or commonly known as channel state information (CSI). The principle component analysis (PCA) technique is used to reduce the estimates dimension. After that FrFT (fractional Fourier transform) is applied to analyse the frequency-time relationship, i.e. to check whether it is separable for different scenarios or not.

Sensing performance of commensal for a particular object changes with its distance from the receiver. Firstly, this system estimates the channel state information (CSI) from the received telecom signal. Secondly, it predicts and evaluates the environmental changes from the change in the channel characteristics.

Two types of input signals are required, i.e. there will be two different processing chains. The first one is used when real-time input data is coming from UE/receiver installed in the environment. The second chain is required when the central processor sets the processing and information depending on the use-case of the LTE CommSense. In the next stage, the CSIs are used to attain knowledge about the environment by an NN classifier. PCA is used to reduce dimension. The objective of this phase is to create the usefulness of detecting objects like human targets in an indoor/outdoor scenarios using cluster analysis. An average recognition of object/human with an accuracy of 88.9% has been achieved. It can be used for classification of different objects like car, bike, etc. The range resolution varies in the LTE Commensal radar case with minimum being 0.5 m. Velocity resolution has not been considered so far for LTE Commensal radar. Even though it has poor resolution but with the use of AI techniques, the accuracy as well as classification has been improved in both indoor and outdoor scenarios. Commensal radar is more suitable for applications where range resolution is not a major concern.

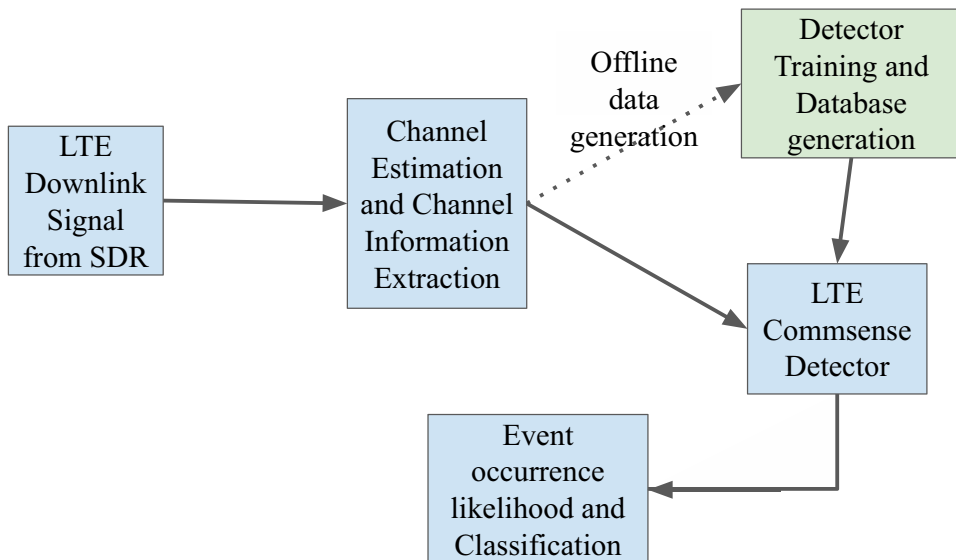


Figure 15. LTE commensal radar working principle.

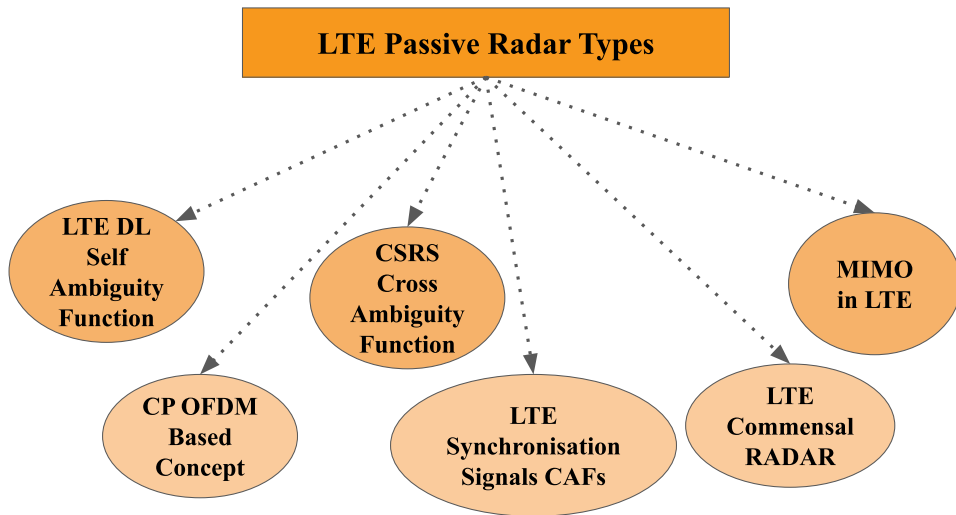


Figure 16. Summary of the types of LTE passive RADAR.

Figure 16 and Table 3 summarize the various types of LTE-based passive RADARs.

6. Introduction to 5 G-NR RADAR

Because 5 G NR radio packets are nearly identical to 4 G LTE radio packets, the LTE passive radio system will find it easier to transition to 5 G passive radar. Additionally, increased bandwidth and MIMO capabilities will eventually improve the properties of passive radar. In Baquero Barneto et al. (2019), the type of processing principles, implementation challenges, and performance of OFDM radars on base stations of 4 G LTE and 5 G-NR has been evaluated with their usage for surveillance applications. Range-Velocity estimation and target detection performance has been done using simulations. It has been reported that 5 G-NR waveforms through their configurable sub-carrier spacing & bandwidth gives a good sensing performance which is quite intuitive as the resolution improves with more bandwidth. The 5 G Tx-Rx are considered for OFDM radar case specifically on shared antenna case. The channel bandwidth of 100 MHz is used to provide better sensing below 6 GHz frequency range. The accuracy for range estimation has been around 1 m and even at lower SNR like -30 dB, the detection probability of object has been around 90%.

In Thoma et al. (2019) a new radar service known as cooperative passive coherent location (CPCL) has been proposed. It is a type of MIMO radar which is for public user groups offered by mobile network. The CPCL extends the passive radar idea by establishing cooperative principles which takes advantage of 4 G LTE & 5 G NR systems. SDRs are used for synchronous radio signalling which is then fused with radar data. CPCL promises to be an ever-present radar service which is re-configurable and adaptive. It is also considered as a green technology because it uses full radio resource, i.e. full frequency band and hardware. The idea of CPCL method came from the vehicle to vehicle (V2X) communication, and it can also be used in different applications like in logistics service, UAVs, transport service and in security applications.

Table 3. Summary of the types of LTE passive radars.

LTE passive radar types	Technology used for LTE passive radar	Authors	Advantages
LTE DL Self Ambiguity Function	Whole LTE downlink signal is used for passive detection	3rd Generation Partnership Pro (2010), Dan et al. (2019); Evers and Jackson (2014a); Raja Abdullah et al. (2015); Salah et al. (2013)	Best range & velocity resolution
CP OFDM-based concept	Only CP-OFDM property of LTE is used for passive detection	Berger et al. (2008), (2010); Xiaoqi Yang et al. (2016)	Low processing time
CSRS Cross-Ambiguity Function	Properties of LTE-CSRS is used for passive detection	Dan et al. (2018); Evers and Jackson (2014b)	Less hardware and complexity but have poor range and velocity resolution
Synchronization Signals CAFs	Properties of LTE-SS is used for passive detection	Evers and Jackson (2014b)	Less hardware and complexity but have poor range and velocity resolution
MIMO in LTE	MIMO properties of LTE is used for passive detection	Bliss and Forsythe (2003); Fishler et al. (2004); Khawar, Abdel-Hadi, and Clancy (2014)	More hardware and complex but have best range and velocity resolution
LTE Commensal Radar	CSI collections and environment sensing	Sardar, Mishra, and Khan (2017, 2018a, 2020)	Have good range resolution but velocity resolution is not reported

A 5 G-NR Radar which uses same OFDM structure for both radar and telecommunication purpose with same spectral efficiency and transmit energy has been proposed in Kiviranta, Moilanen, and Roivainen (2019). Radio frame duration of 10 ms has been considered and it consists of ten sub-frames of 1 ms in both 4 G-LTE & 5 G-NR (3rd Generation Partnership Project 2010). The sub-frames have two slots consists of 14 consecutive symbols. The slots duration is in milliseconds, and also depends upon symbol time adjustment which is obtained by identifying PSS & SSS like synchronization signals (E. Parkvall, Dahlman, and Sköld. 2018; M Krátký and Fuxa 2015). These synchronization signals can be used for object detection and range estimation as seen in Section 5.4.4. The PSS is a 127 length m-sequence in frequency domain, it relaxes the ambiguity problem of time and frequency offset created by Zadoff Chu sequence and particularly in LTE case. However, the 5 G case is quite different from LTE as a synchronization signal block (SSB) consisting of 4 symbols exists in 5 G-NR. A burst of synchronization signal blocks (SSBs) can be transmitted (depends upon frequency range and sub-carrier spacing) which is claimed to be a solution of problem created by Zadoff Chu sequence (PSS/SSS). Frequency offset has a greater impact on property of auto-correlation which has to be resolved before the SSS and PSS detection. The simulation model is shown in Figure 17 without synchronization loop and frequency error as considered in Kiviranta, Moilanen, and Roivainen (2019). When the peak at correlation output of PSS block is observed, the range is assumed to be a round trip time from radar to object to radar (which is monotonic radar case), for passive radar case we have. Also, with the use of frequency estimate block, object velocity can be calculated when PSS correlation peak is detected. Frequency offset estimation is done by cyclic prefix (CP) correlation, Which is elaborated as follows: In estimator block, the correlation is taken between the 5 G-OFDM received signal with its delayed version of fast Fourier transform (FFT). After that the output is integrated across

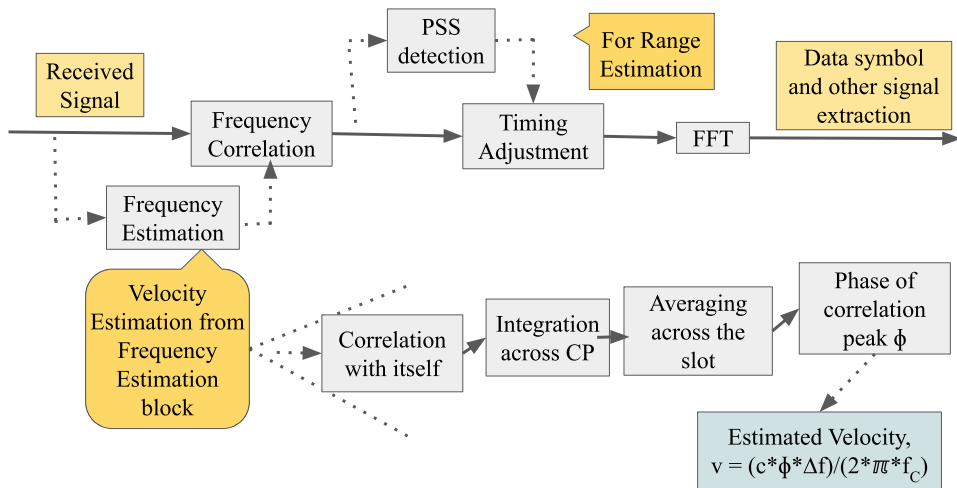


Figure 17. A prototype of 5 G radar.

all parts of symbols (including CP) and averaged over the slot. From the strongest correlation peak, phase ϕ is obtained which is used to estimate frequency offset. Rest of the radar processing is similar to the previously discussed methods for range, velocity, RD map, etc.

In Barneto et al. (2019), similar work as seen in LTE DL self ambiguity radar has been proposed. The whole 5 G signal has been used to sense the object with just spectrum sensing. The system is able to sense objects at a maximum range of 100 m.

7. Discussion & conclusion

Because LTE has two sub-carrier separations, 15 kHz and 7.5 kHz, the sub-carrier is adjusted according to bandwidth without affecting range resolution. When the bandwidth is increased from 1.25 MHz to 20 MHz, the range resolution improves from 120 m to 7.56 m.

Table 3 depicts and compares the waveform properties of currently implemented passive radar base stations of interest for various communication technologies such as FM, DVB-T, GSM, WiFi, and WiMAX (Chetty, Smith, and Woodbridge 2012; Colone, Falcone, and Lombardo 2010, 2012; Dan et al. 2018; Evers and Jackson 2014a; Feng et al. 2019; Guo, Woodbridge, and Baker 2008; Howland, Maksimiuk, and Reitsma 2005; Jishy et al. 2010; Saini and Cherniakov 2005; Tan et al. 2005a; Wang, Hou, and Lu 2009a,b,c). It can be concluded that:

(1) Wide band signals such as LTE, DVB-T, WiFi, WiMAX, and 5 G provide good range resolution. MIMO, on the other hand, improves the properties of LTE passive radar, making it a better choice.

(2) LTE and 5 G provide the best velocity resolution when compared to WiFi and WiMAX.

(3) In terms of coverage area, LTE can cover tens of metres (pico and femto cells) and up to ten kilometres (macrocell). Thus, LTE can cover a wide range and is regarded as

a suitable wide range passive radar, i.e. in the blind spot of an LTE network, the direct path signal can be selected from the nearest base station.

(4) Because of their lower hardware and implementation complexity, CSRS and SS-based cross ambiguity processing techniques are preferred in terms of processing time in LTE passive radar performance.

Based on these discussions, it is possible to conclude that LTE passive radar is a practical, cost-effective, and simple-to-implement technology. More research is needed to fully utilize the resource block and other technical aspects when it is upgraded to 5 G-based passive RADAR.

Many potential applications for LTE passive Radars, such as automation industry, smart city surveillance, self driving, autonomous cars UAVs/UGVs/Drones, and smart parking, have yet to be investigated. Furthermore, 5 G-NR research and implementation are progressing, and it is likely that 4 G-LTE passive radar will be replaced or inherited by 5 G-NR-based passive radar. Because 5 G is an improved version of 4 G, passive radar technology transfer will be simple to implement for various usage scenarios.

Acknowledgements

This work was supported by the INCAPS project: 287918 of the INTPART program, the LUCAT project: 280835 of the IKTPLUSS program from the Research Council of Norway, and the Department of Science and Technology (DST), Govt. of India (Ref. No. INT/NOR/RCN/ICT/P-01/2018).

Disclosure statement

No potential conflict of interest was reported by the author(s).

Funding

This work was supported by the INCAPS project: 287918 of INTPART program from the Research Council of Norway and the Low-Altitude UAV Communication and Tracking (LUCAT) project: 280835 of the IKTPLUSS program from the Research Council of Norway.

ORCID

Linga Reddy Cenkeramaddi  <http://orcid.org/0000-0002-1023-2118>

References

- 3rd Generation Partnership Project. 2010. Technical Specification Group Radio Access Network; Evolved Universal Terrestrial Radio Access (E-utra); Physical Channels and Modulation, Release 8, 3gpp Ts 36.211. ETSI.
- Abdullah, R. S. A. R., F. Hashim, A. Salah, N. U. R. EMILEEN RASHID, A. Ismail, and H. Aziz. 2015. "Experimental Investigation on Target Detection and Tracking in Passive Radar Using Long-term Evolution Signal." *IET Radar, Sonar Navigation* 10 (9). doi:10.1049/iet-rsn.2015.0346.
- Baquero Barneto, C., T. Riihonen, M. Turunen, L. Anttila, M. Fleischer, K. Stadius, J. Ryyänen, and M. Valkama. 2019. "Full-duplex Odfm Radar with Lte and 5g Nr Waveforms: Challenges, Solutions, and Measurements." *IEEE Transactions on Microwave Theory and Techniques* 670 (10): 4042–4054. doi:10.1109/TMTT.2019.2930510.

- Barneto, C. B., M. Turunen, S. D. Liyanaarachchi, L. Anttila, A. Brihuega, T. Riihonen, and M. Valkama. 2019. "High-accuracy Radio Sensing in 5g New Radio Networks: Prospects and Self-interference Challenge." In *2019 53rd Asilomar Conference on Signals, Systems, and Computers*, 1159–1163. Pacific Grove, CA, USA. doi: [10.1109/IEEECONF44664.2019.9048786](https://doi.org/10.1109/IEEECONF44664.2019.9048786).
- Berger, C. R., B. Demissie, J. Heckenbach, P. Willett, and S. Zhou. 2010. "Signal Processing for Passive Radar Using Ofdm Waveforms." *IEEE Journal of Selected Topics in Signal Processing* 40 (1): 226–238. doi:[10.1109/JSTSP.2009.2038977](https://doi.org/10.1109/JSTSP.2009.2038977).
- Berger, C. R., S. Zhou, P. Willett, B. Demissie, and J. Heckenbach. 2008. "Compressed Sensing for Ofdm/mimo Radar." In *2008 42nd Asilomar Conference on Signals, Systems and Computers*, 213–217. Pacific Grove, CA, USA. doi: [10.1109/ACSSC.2008.5074394](https://doi.org/10.1109/ACSSC.2008.5074394).
- Blázquez-García, R., J. Casamayón-Antón, and M. Burgos-García. 2018. "Lte-r Based Passive Multistatic Radar for High-speed Railway Network Surveillance." In *2018 15th European Radar Conference (EuRAD)*, 6–9. Madrid, Spain. doi: [10.23919/EuRAD.2018.8546516](https://doi.org/10.23919/EuRAD.2018.8546516).
- Bliss, D. W., and K. W. Forsythe. 2003. "Multiple-input Multiple-output (Mimo) Radar and Imaging: Degrees of Freedom and Resolution." In *The Thirty-Seventh Asilomar Conference on Signals, Systems Computers, 2003*, volume 1, 54–59. Pacific Grove, CA, USA. doi: [10.1109/ACSSC.2003.1291865](https://doi.org/10.1109/ACSSC.2003.1291865).
- Chabriel, G., J. Barrère, G. Gassier, and F. Briolle. 2014. "Passive Covert Radars Using Cp-ofdm Signals. A New Efficient Method to Extract Targets Echoes." In *2014 International Radar Conference*, 1–6. Lille, France. doi: [10.1109/RADAR.2014.7060382](https://doi.org/10.1109/RADAR.2014.7060382).
- Chetty, K., G. E. Smith, and K. Woodbridge. 2012. "Through-the-wall Sensing of Personnel Using Passive Bistatic Wifi Radar at Standoff Distances." *IEEE Transactions on Geoscience and Remote Sensing* 500 (4): 1218–1226. doi:[10.1109/TGRS.2011.2164411](https://doi.org/10.1109/TGRS.2011.2164411).
- Coleman, C. J., R. A. Watson, and H. Yardley. 2008. "A Practical Bistatic Passive Radar System for Use with Dab and Dm Illuminators." In *2008 IEEE Radar Conference*. Rome, Italy, 1–6. doi: [10.1109/RADAR.2008.4721007](https://doi.org/10.1109/RADAR.2008.4721007).
- Colone, F., P. Falcone, C. Bongioanni, and P. Lombardo. 2012. "Wifi-based Passive Bistatic Radar: Data Processing Schemes and Experimental Results." *IEEE Transactions on Aerospace and Electronic Systems* 480 (2): 1061–1079. doi:[10.1109/TAES.2012.6178049](https://doi.org/10.1109/TAES.2012.6178049).
- Colone, F., P. Falcone, and P. Lombardo. 2010. "Ambiguity Function Analysis of Wimax Transmissions for Passive Radar." In *2010 IEEE Radar Conference*. Arlington, VA, USA, 689–694. doi: [10.1109/RADAR.2010.5494533](https://doi.org/10.1109/RADAR.2010.5494533).
- Costas, J. P. 1984. "A Study of A Class of Detection Waveforms Having Nearly Ideal Range—doppler Ambiguity Properties." *Proceedings of the IEEE* 720 (8): 996–1009. doi:[10.1109/PROC.1984.12967](https://doi.org/10.1109/PROC.1984.12967).
- Dan, Y., X. Wan, J. Yi, and Y. Rao. 2018. "Ambiguity Function Analysis of Long Term Evolution Transmission for Passive Radar." In *2018 12th International Symposium on Antennas, Propagation and EM Theory (ISAPE)*. Hangzhou, China, 1–4, doi: [10.1109/ISAPE.2018.8634255](https://doi.org/10.1109/ISAPE.2018.8634255).
- Dan, Y., Y. Jianxin, X. Wan, Y. Rao, and B. Wang. 2019. "Lte-based Passive Radar for Drone Detection and Its Experimental Results." *The Journal of Engineering* 2019 (7): 6910–6913. doi:[10.1049/joe.2019.0583](https://doi.org/10.1049/joe.2019.0583).
- De Quevedo, Á. D., F. I. Urzaiz, J. G. Menoyo, and A. A. López. 2018. "Drone Detection and Rcs Measurements with Ubiquitous Radar." In *2018 International Conference on Radar (RADAR)*. Brisbane, QLD, Australia, 1–6. doi: [10.1109/RADAR.2018.8557320](https://doi.org/10.1109/RADAR.2018.8557320).
- Evers, A., and J. A. Jackson. Experimental Passive Sar Imaging Exploiting Lte, Dvb, and Dab Signals. In *2014 IEEE Radar Conference*, 680–685, 2014a. doi: [10.1109/RADAR.2014.6875677](https://doi.org/10.1109/RADAR.2014.6875677).
- Evers, A., and J. A. Jackson. 2014b. "Analysis of an Lte Waveform for Radar Applications." In *2014 IEEE Radar Conference*. Cincinnati, Ohio, USA, 200–205, doi: [10.1109/RADAR.2014.6875584](https://doi.org/10.1109/RADAR.2014.6875584).
- Fang, G., J. Yi, X. Wan, Y. Liu, and H. Ke. 2018. "Experimental Research of Multistatic Passive Radar with a Single Antenna for Drone Detection." *IEEE Access* 6: 33542–33551. doi:[10.1109/ACCESS.2018.2844556](https://doi.org/10.1109/ACCESS.2018.2844556).
- Feng, W., J. Friedt, H. Zhipeng, G. Cherniak, and M. Sato. 2019. "Wifi-based Imaging for Ground Penetrating Radar Applications: Fundamental Study and Experimental Results." *The Journal of Engineering* 2019 (5): 6364–6368. doi:[10.1049/joe.2019.0209](https://doi.org/10.1049/joe.2019.0209).

- Fishler, E., A. Haimovich, R. Blum, D. Chizhik, L. Cimini, and R. Valenzuela. 2004. "Mimo Radar: An Idea Whose Time Has Come." In *Proceedings of the 2004 IEEE Radar Conference (IEEE Cat. No.04CH37509)*. Philadelphia, PA, USA, 71–78, doi: [10.1109/NRC.2004.1316398](https://doi.org/10.1109/NRC.2004.1316398).
- Gesbert, D., M. Shafi, D.-S. Shiu, P. J. Smith, and A. Naguib. 2003. "From Theory to Practice: An Overview of Mimo Space-time Coded Wireless Systems." *IEEE Journal on Selected Areas in Communications* 210 (3): 281–302. doi:[10.1109/JSAC.2003.809458](https://doi.org/10.1109/JSAC.2003.809458).
- Gómez-del-Hoyo, P., J. L. Bárcena-Humanes, D. Mata-Moya, D. Juara-Casero, and V. Jiménez-de-Lucas. 2015. "Passive Radars as Low Environmental Impact Solutions for Smart Cities Traffic Monitoring." *IEEE EUROCON 2015 - International Conference on Computer as a Tool (EUROCON)* 1–6. doi:[10.1109/EUROCON.2015.7313780](https://doi.org/10.1109/EUROCON.2015.7313780).
- Guo, H., K. Woodbridge, and C. J. Baker. 2008. "Evaluation of Wifi Beacon Transmissions for Wireless Based Passive Radar." In *2008 IEEE Radar Conference*. Rome, Italy, 1–6. doi: [10.1109/RADAR.2008.4720810](https://doi.org/10.1109/RADAR.2008.4720810).
- Hack, D. E. "Passive MIMO Radar Detection." PhD thesis, AFIT, 2013.
- Haisheng, X., R. S. Blum, J. Wang, and J. Yuan. 2015a. "Colocated Mimo Radar Waveform Design for Transmit Beampattern Formation." *IEEE Transactions on Aerospace and Electronic Systems* 510 (2): 1558–1568. doi:[10.1109/TAES.2014.140249](https://doi.org/10.1109/TAES.2014.140249).
- Haisheng, X., J. Wang, J. Yuan, and X. Shan. 2015b. "Colocated Mimo Radar Transmit Beamspace Design for Randomly Present Target Detection." *IEEE Signal Processing Letters* 22 (7): 828–832. doi:[10.1109/LSP.2014.2371241](https://doi.org/10.1109/LSP.2014.2371241).
- Howland, P. E., D. Maksimiuk, and G. Reitsma. 2005. "Fm Radio Based Bistatic Radar." *IEE Proceedings - Radar, Sonar and Navigation* 152 (7): 107–115. doi:[10.1049/ip-rsn:20045077](https://doi.org/10.1049/ip-rsn:20045077).
- Jack Gough and Great Britain. 1993. *Watching the Skies: A History of Ground Radar for the Air Defence of the United Kingdom by the Royal Air Force from 1946 to 1975*/Jack Gough. H.M.S.O London: ISBN 0117727237.
- Jian, M., Z. Lu, and V. C. Chen. 2018. "Drone Detection and Tracking Based on Phase-interferometric Doppler Radar." In *2018 IEEE Radar Conference (RadarConf18)*. Oklahoma City, OK, USA, 1146–1149. doi: [10.1109/RADAR.2018.8378723](https://doi.org/10.1109/RADAR.2018.8378723).
- Jishy, K., F. Lehmann, M. Moruzzis, F. Gosselin, and G. Salut. 2010. "Tracking Maneuvering Target with Particle Filter Techniques on Passive Radar Using Fm and Dvbt Broadcasting Signals." In *2010 IEEE Radar Conference*. Arlington, VA, USA, 642–646. doi: [10.1109/RADAR.2010.5494544](https://doi.org/10.1109/RADAR.2010.5494544).
- Khawar, A., A. Abdel-Hadi, and T. C. Clancy. 2014. "Spectrum Sharing between S-band Radar and Lte Cellular System: A Spatial Approach." In *2014 IEEE International Symposium on Dynamic Spectrum Access Networks (DYSPAN)*. McLean, VA, USA, 7–14. doi: [10.1109/DySPAN.2014.6817773](https://doi.org/10.1109/DySPAN.2014.6817773).
- Kiviranta, M., I. Moilanen, and J. Roivainen. 2019. "5g Radar: Scenarios, Numerology and Simulations." In *2019 International Conference on Military Communications and Information Systems (ICMCIS)*. Budva, Montenegro, 1–6. doi: [10.1109/ICMCIS.2019.8842780](https://doi.org/10.1109/ICMCIS.2019.8842780).
- Krátký, M., and L. Fuxa. 2015. "Mini Uavs Detection by Radar." In *International Conference on Military Technologies (ICMT) 2015*. Brno, Czech Republic, 1–5, doi: [10.1109/MILTECHS.2015.7153647](https://doi.org/10.1109/MILTECHS.2015.7153647).
- Kuschel, H., J. Heckenbach, S. Muller, and R. Appel. 2008. "On the Potentials of Passive, Multistatic, Low Frequency Radars to Counter Stealth and Detect Low Flying Targets." In *2008 IEEE Radar Conference*. Rome, Italy, 1–6. doi: [10.1109/RADAR.2008.4720984](https://doi.org/10.1109/RADAR.2008.4720984).
- Kwon, O.-Y., R. Song, M. Yu-Zhen, and B.-S. Kim. 2016. "Integrated Mimo Antennas for Lte and V2v Applications." *2016 URSI Asia-Pacific Radio Science Conference (URSI AP-RASC)*. Seoul, Korea (South), 8: 1057–1060. doi:[10.1109/URSIAP-RASC.2016.7601146](https://doi.org/10.1109/URSIAP-RASC.2016.7601146).
- Levanon, N., and E. Mozeson. 2004. *Radar Signals*. Hoboken, NJ: John Wiley & Sons.
- Li, K., C. Yuen, S. S. Kanhere, K. Hu, W. Zhang, F. Jiang, and X. Liu. 2019. "An Experimental Study for Tracking Crowd in Smart Cities." *IEEE Systems Journal* 130 (3): 2966–2977. doi:[10.1109/JSYST.2018.2880028](https://doi.org/10.1109/JSYST.2018.2880028).
- Liu, Y., X. Wan, H. Tang, J. Yi, Y. Cheng, and X. Zhang. 2017. "Digital Television Based Passive Bistatic Radar System for Drone Detection." In *2017 IEEE Radar Conference (RadarConf)*. Seattle, WA, USA, 1493–1497. doi: [10.1109/RADAR.2017.7944443](https://doi.org/10.1109/RADAR.2017.7944443).

- Min, S., and C. L. Nikias. 1994. "An ML/mmse Estimation Approach to Blind Equalization." In *Proceedings of ICASSP '94. IEEE International Conference on Acoustics, Speech and Signal Processing*. Adelaide, SA, Australia, vol.4, IV/569–IV/572. doi: [10.1109/ICASSP.1994.389753](https://doi.org/10.1109/ICASSP.1994.389753).
- Mueller, S., J. Schell, M. Glende, J. Heckenbach, and C. Schumacher. 2007. "Experimental Passive Radar Systems Using Digital Illuminators (Dab/dvb-t)." In *International Radar Symposium (IRS 2007)*. Cologne, Germany, 411–417.
- Parkvall, S., E. Dahlman, and J. Sköld. 2018. *5G NR: The Next Generation Wireless Access Technology*. United States: Academic Press.
- Petri, D., C. Moscardini, M. Martorella, M. Conti, A. Capria, and F. Berizzi. 2012. "Performance Analysis of the Batches Algorithm for Range-doppler Map Formation in Passive Bistatic Radar." In *IET International Conference on Radar Systems (Radar 2012)*. Glasgow, UK, 1–4. doi: [10.1049/cp.2012.1570](https://doi.org/10.1049/cp.2012.1570).
- Richard, M. A. 2014. "Fundamentals of Radar Signal Processing." Tata McGraw-Hill Education
- Saini, R., and M. Cherniakov. 2005. "Dtv Signal Ambiguity Function Analysis for Radar Application." *IEE Proceedings - Radar, Sonar and Navigation* 152 (7): 133–142. doi:[10.1049/ip-rsn:20045067](https://doi.org/10.1049/ip-rsn:20045067).
- Salah, A. A., R. S. A. R. Abdullah, A. Ismail, F. Hashim, C. Y. Leow, M. B. Roslee, and N. E. A. Rashid. 2013. "Feasibility Study of Lte Signal as a New Illuminators of Opportunity for Passive Radar Applications." In *2013 IEEE International RF and Microwave Conference (RFM)*. Penang, Malaysia, 258–262. doi: [10.1109/RFM.2013.6757261](https://doi.org/10.1109/RFM.2013.6757261).
- Sardar, S., A. K. Mishra, and M. Z. A. Khan. 2017. "Lte-commsense System and Its Feasibility Analysis." In *2017 IEEE AFRICON*. Cape Town, South Africa, 1564–1568. doi: [10.1109/AFRCON.2017.8095715](https://doi.org/10.1109/AFRCON.2017.8095715).
- Sardar, S., A. K. Mishra, and M. Z. A. Khan. 2018a. "Lte Commsense for Object Detection in Indoor Environments." *IEEE Aerospace and Electronic Systems Magazine* 330 (7): 46–59. doi:[10.1109/MAES.2017.180054](https://doi.org/10.1109/MAES.2017.180054).
- Sardar, S., A. K. Mishra, and M. Z. A. Khan. 2020. "Performance Evaluation of Lte-commsense System for Discriminating the Presence of Multiple Objects in Outdoor Environment." *IEEE Transactions on Instrumentation and Measurement* 690 (3): 760–769. doi:[10.1109/TIM.2019.2904332](https://doi.org/10.1109/TIM.2019.2904332).
- Sardar, S., B. A. G. Ravi Sharan, P. K. Rai, G. Kumar, M. Z. Ali Khan, and A. K. Mishra. 2018b. "Indoor Localization System Using Commensal Radar Principle." In *2018 Progress in Electromagnetics Research Symposium (PIERS-Toyama)*. Toyama, Japan, 751–755. doi: [10.23919/PIERS.2018.8597686](https://doi.org/10.23919/PIERS.2018.8597686).
- Sonny, A., P. K. Rai, A. Kumar, and M. Z. A. Khan. 2020. "Deep Learning-based Smart Parking Solution Using Channel State Information in Lte-based Cellular Networks." In *2020 International Conference on COMmunication Systems NETworks (COMSNETS)*. Bangalore, India, 642–645. doi: [10.1109/COMSNETS48256.2020.9027447](https://doi.org/10.1109/COMSNETS48256.2020.9027447).
- Swords, S. S. 1986. "Technical History of the Beginnings of Radar." History of Technology. Institution of Engineering and Technology, <https://digital-library.theiet.org/content/books/ht/pbht006e>.
- Tan, D., H. Sun, Y. Lu, M. Lesturgie, and C. H. Lim. 2005a. "Passive Radar Using Global System for Mobile Communication Signal: Theory, Implementation and Measurements." *IEE Proceedings - Radar, Sonar and Navigation* 152 (3): 116–123. doi:[10.1049/ip-rsn:20055038](https://doi.org/10.1049/ip-rsn:20055038).
- Tan, D., H. Sun, Y. Lu, M. Lesturgie, and C. H. Lim. 2005b. "Passive Radar Using Global System for Mobile Communication Signal: Theory, Implementation and Measurements." *IEE Proceedings - Radar, Sonar and Navigation* 152 (3): 116–123. doi:[10.1049/ip-rsn:20055038](https://doi.org/10.1049/ip-rsn:20055038).
- Thoma, R. S., C. Andrich, G. D. Galdo, M. Dobereiner, M. A. Hein, M. Kaske, G. Schafer, et al. 2019. "Cooperative Passive Coherent Location: A Promising 5g Service to Support Road Safety." *IEEE Communications Magazine* 570 (9): 86–92. doi:[10.1109/MCOM.001.1800242](https://doi.org/10.1109/MCOM.001.1800242).
- Vinogradov, E., D. A. Kovalev, and S. Pollin. 2018a. "Simulation and Detection Performance Evaluation of a Uav-mounted Passive Radar." In *2018 IEEE 29th Annual International Symposium on Personal, Indoor and Mobile Radio Communications (PIMRC)*. Bologna, Italy, 1185–1191. doi: [10.1109/PIMRC.2018.8580940](https://doi.org/10.1109/PIMRC.2018.8580940).
- Vinogradov, E., D. A. Kovalev, and S. Pollin. 2018b. "Simulation and Detection Performance Evaluation of a Uav-mounted Passive Radar." In *2018 IEEE 29th Annual International Symposium on Personal, Indoor and Mobile Radio Communications (PIMRC)*, 1185–1191. doi: [10.1109/PIMRC.2018.8580940](https://doi.org/10.1109/PIMRC.2018.8580940).

- Wan, X., J. Yi, Z. Zhao, and H. Ke. 2014. "Experimental Research for Cmmmb-based Passive Radar under a Multipath Environment." *IEEE Transactions on Aerospace and Electronic Systems* 500 (1): 70–85. doi:[10.1109/TAES.2013.120737](https://doi.org/10.1109/TAES.2013.120737).
- Wang, Q., C. Hou, and Y. Lu. 2009a. "Wimax Signal Waveform Analysis for Passive Radar Application." In *2009 International Radar Conference "Surveillance for a Safer World"*, 1–6.
- Wubben, D., R. Bohnke, V. Kuhn, and K. Kammeyer. 2003. "Mmse Extension of V-blast Based on Sorted Qr Decomposition." In *2003 IEEE 58th Vehicular Technology Conference. VTC 2003-Fall (IEEE Cat. No.03CH37484)*. Orlando, FL, USA, volume 1, 508–512. doi: [10.1109/VETECF.2003.1285069](https://doi.org/10.1109/VETECF.2003.1285069).
- Xu, Y., X. Di, Z. Zhang, L. Li, and J. Tian. 2019. Millimeter-wave Multi-radar System for Ubiquitous Concealed Dangerous Object Detection. In *2019 IEEE SmartWorld, Ubiquitous Intelligence Computing, Advanced Trusted Computing, Scalable Computing Communications, Cloud Big Data Computing, Internet of People and Smart City Innovation (SmartWorld/SCALCOM/UIC/ATC/CBDCom/IOP/SCI)*. Leicester, UK, 1896–1900. doi: [10.1109/SmartWorld-UIC-ATC-SCALCOM-IOP-SCI.2019.00333](https://doi.org/10.1109/SmartWorld-UIC-ATC-SCALCOM-IOP-SCI.2019.00333).
- Yang, X., K. Huo, W. Jiang, J. Zhao, and Z. Qiu. 2016. A Passive Radar System for Detecting Uav Based on the Ofdm Communication Signal. In *2016 Progress in Electromagnetic Research Symposium (PIERS)*. Shanghai, China, 2757–2762. doi: [10.1109/PIERS.2016.7735118](https://doi.org/10.1109/PIERS.2016.7735118).